The lecture is based on
doctoral dissertation of

Katarzyna Kubicka, M.Sc.

FIRE SAFETY ASSESSMENT OF STEEL TRUSS STRUCTURES A PROBABILISTIC APPROACH

Supervisor: Urszula Radoń, Ph.D, D.Sc., KUT Professor
Auxiliary supervisor: Urszula Pawlak, Ph.D.
Kielce 2017

In the course of fire steel parameters are subjected to degradation due to high temperature action, it leads to load-carrying capacity decrement of distinct structural elements.

Such a situation may lead to **failure or structural collapse**.

In the case of fire **life protection** is an absolutely primary concern.

In structural design **it is necessary to assure a relevant fire protection class**, in order to assure an appropriately long escape time for humans.

The next vital issue is assuring a post-fire ability of a structure to function, introducing a maximum limitation of necessary repair works.

Steel structures subjected to fire are bound to rapidly collapse.

A catastrophic case concerns the steel hall in Lubań, Polish Upper Silesia

In July 2012 the hall was demolished in only 17 minutes

View of a portal frame column subjected to fire [51]

Fire events of the Łazienkowski Bridge in Warsaw, February 2015

A displaced bearing on the edge support of Łazienkowski Bridge

Fire at the Gdańsk Shipyard Hall, November 1994
(Fakt24.pl, 2015-11-24) the author: Alina Żakowska

On 24th of November, 1994 in the Gdańsk Shipyard Hall an event was planned. The first act to play was Golden Life, the rock band from Gdańsk, next, a live transmossion from Berlin MTV Music Awards was about to come. An hour after the Golden Life show a fire burst in.

Seven people were killed, an approx. number of 300 injured.

When the fire burst in the audience sector the spectators ran towards the exit in panic.
The terrified crowd of approx. 800 persons was blocked in the main exit, due to its partial clearance only because of the steel bar grid, constraining the passage.
The most devastating factor was a sudden fire blast, which exploded when the firefighters opened the windows.


©Agencja Gazeta

Conclusion. In steel structure design it is necessary to provide an appropriate fire resistance class, assuring a sufficient structural load-carrying capacity in order to evacuate the people safely and extinguish the fire before the event of structural damage threatening human life

The joint action of two fields: fire analysis and reliability assessment

The most challenging issue here is **working a relevant probabilistic model valid in fire conditions**

Uncertainty origin (three sources):

- fire description – room geometry, the amount and layout of flammable materials, the temperature of exhaust gases
- thermal response of a structure (material properties, boundary conditions, structural temperature)
- mechanical response of a structure

Assuming a proper reliability index is a key issue here.
The majority of steel structures is assumed $\beta = 3{,}8$, while a 50-year structural operation is taken into account.

While fire conditions are addressed the proposed reliability indices take the range 2,5-3,5.

Assumptions linked with heat issues:

- analysis of a developed fire phase, showcasing fire gas temperature in an entire room;
- fire effects reflected by the so-called standard curve
- fire gases acting on every wall of a section;
- uniform temperature distribution in a section;
- regarding thermal and mechanical paramter variation of the material (steel) due to fire,
- thermal parameter variation of insulating materials neglected .

Assumptions linked with mechanical issues:

- geometric linearity;
- structures prevented from stability loss;
- the stress-strain curve in fire conditions sepcified by Eurocode [147];
- rheological impact is neglected

The assumption in reliability analysis:

- the temperature of steel elements and exhaust gases is considered deterministic
- the only random basic variables are cross-sectional characteristics, mechanical parameters of a material and load effects to actions,
- uncorrelated, Gaussian random variables are regarded only

Each civil engineering structure (or element) is assigned the time of its proper function (service) while exposed to fire, not losing its functional features.

This feature is a fire resistance, classified by three following criteria [15]:

- **load-carrying capacity R** – resistance of a load-carrying element to actions;
- **insulation capability I** – the ability of a separating element subjected to one-side fire to limit the temperature growth on the adjacent surfaces
- **tightness E** – the ability of a separating element subjected to one-side fire to limit the crack creation and spreading hot gases into adjacent rooms

Specific heat – the heat amount required for a unit temperature rise of the unit mass of a given body

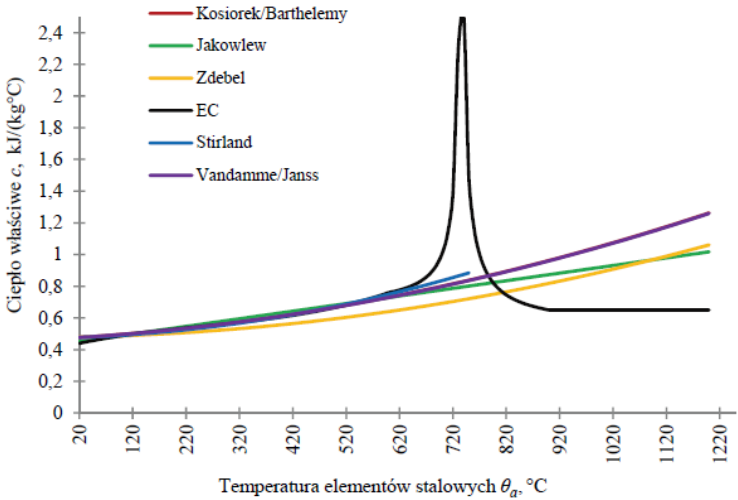

***Rys. 2.1.** Zmiana ciepła właściwego wraz ze wzrostem temperatury*

Fig. 2.1. Variation of specific heat due to temperature rise specific heat temperature of steel elements

The Eurocode curve is distinct, with regard to other curves, by means of a high specific heat peak in temperatures close to 735°C, due to alotropic transformation of iron.

Heat conductivity – a material ability to conduct heat – identical conditions make a higher heat flow in a material of a higher heat conductivity

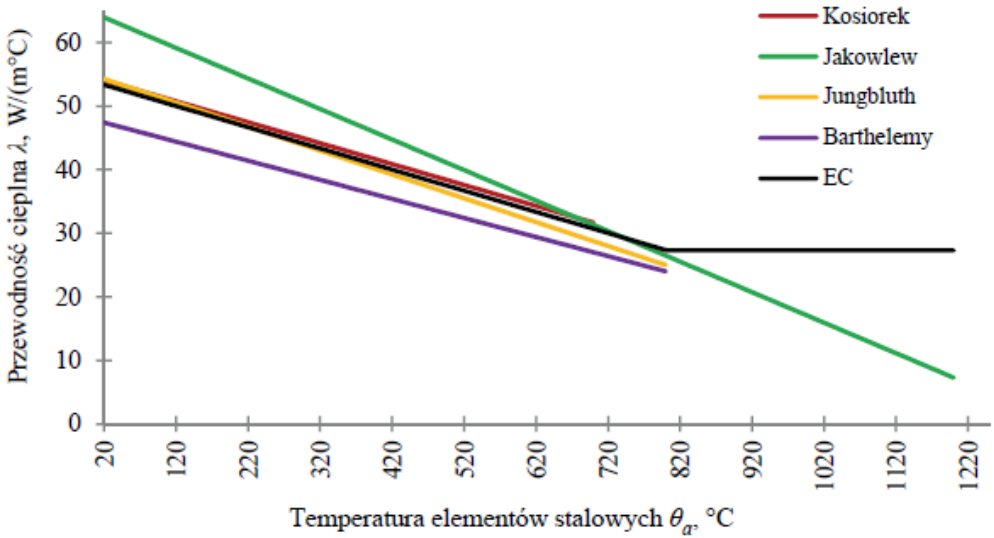

***Rys. 2.2.** Zmiana współczynnika przewodnictwa cieplnego wraz ze wzrostem temperatury*

Fig. 2.2. Variation of heat conductivity due to temperature rise heat conductivity temperature of steel elements

Yield stress – the stress limiting value transforming material into a plastic phase

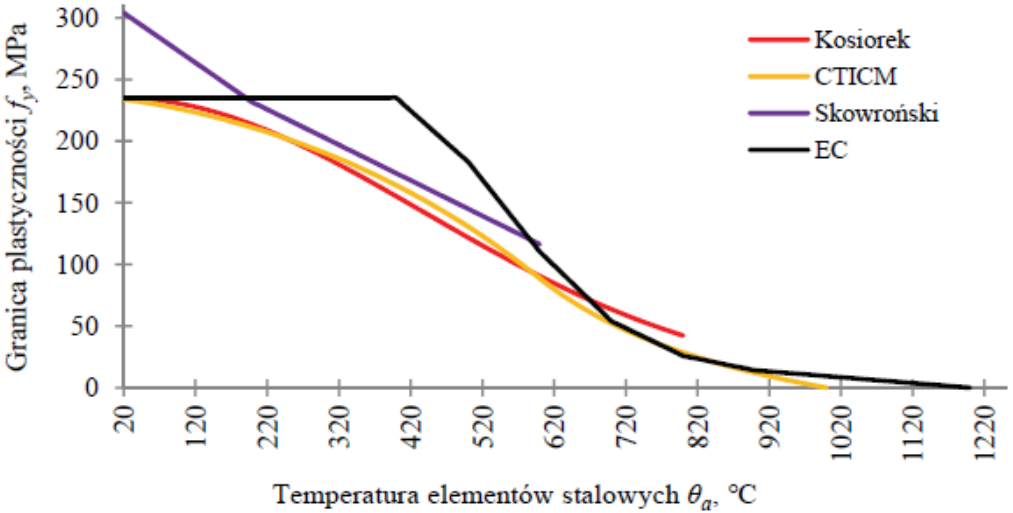

***Rys. 2.3.** Zmiana granicy plastyczności wraz ze wzrostem temperatury*

Fig. 2.3. Variation of yield stress due to temperature rise yield stress temperature of steel elements

Tab. 2.5. Reduction coefficients of yield stress and elasticity modulus

Reduction coefficients in temperature θ_α with respect to f_y or Y in 20 C^o

Reduction coefficient of effective yield stress (with regard to f_y)

Reduction coefficient of linear elasticity modulus (with regard to Y)

Tabela 2.5. Współczynniki redukcyjne granicy plastyczności i modułu sprężystości [147]

Temperatura stali θ_a	Współczynniki redukcyjne przy temperaturze θ_a w stosunku do wartości f_y lub Y w temperaturze 20°C	
	Współczynnik redukcyjny efektywnej granicy plastyczności (w stosunku do f_y) $k_{y,\theta_a} = f_{y,\theta_a} / f_y$	Współczynnik redukcyjny modułu sprężystości liniowej (w stosunku do Y) $k_{E,\theta_a} = Y_{\theta_a} / Y$
20°C	1,000	1,000
100°C	1,000	1,000
200°C	1,000	0,900
300°C	1,000	0,800
400°C	1,000	0,700
500°C	0,780	0,600
600°C	0,470	0,310
700°C	0,230	0,130
800°C	0,110	0,090
900°C	0,060	0,0675
1000°C	0,040	0,0450
1100°C	0,020	0,0225
1200°C	0,000	0,0000

Variation of elasticity modulus caused by temperature rise

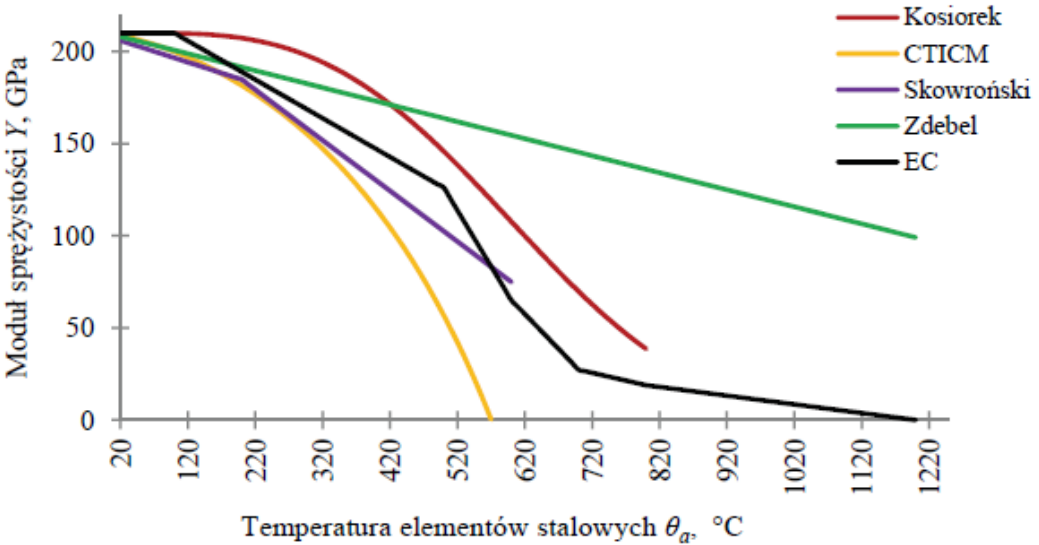

***Rys. 2.4.** Zmiana modułu sprężystości wraz ze wzrostem temperatury*

Fig. 2.4. Variation of elasticity modulus due to temperature rise elasticity modulus temperature of steel elements

Coefficient of thermal expansion

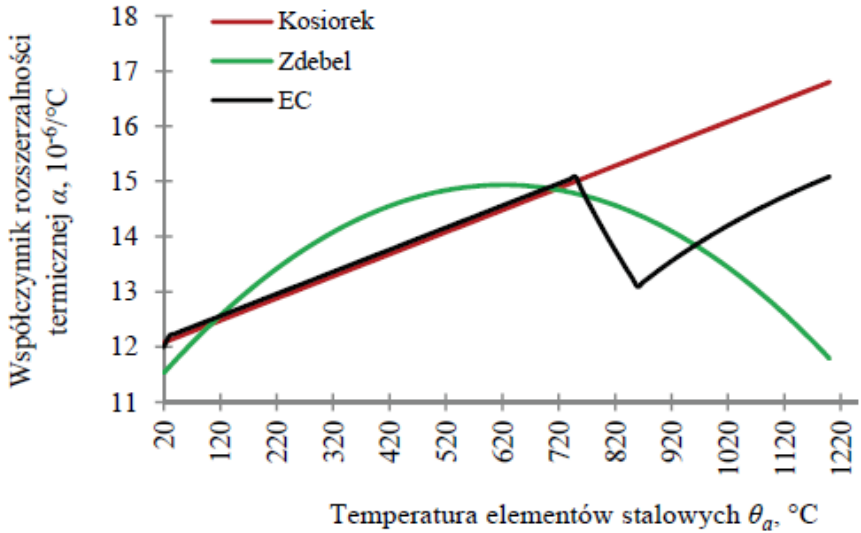

***Rys. 2.5.** Zmiana współczynnika rozszerzalności termicznej wraz ze wzrostem temperatury*

Fig. 2.5. Variation of the coefficient of thermal expansion due to temperature increment temperature of steel elements coefficient of thermal expansion temperature of steel elements

The stress-strain relation of steel at elevated temperatures

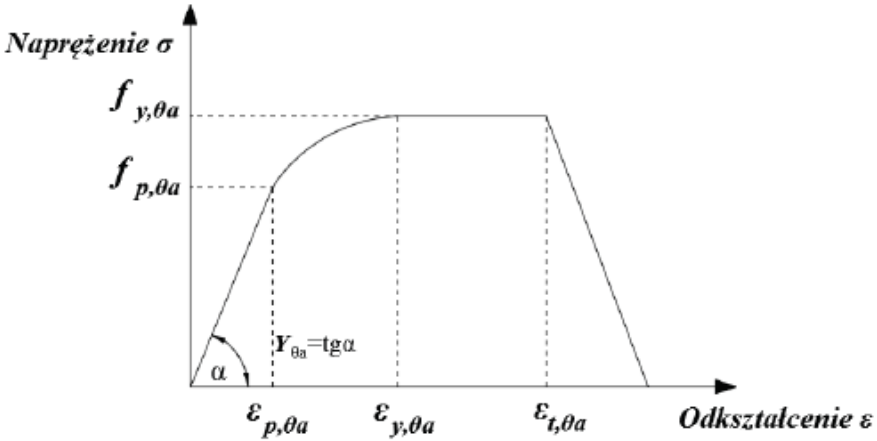

Rys. 2.6. Zależność naprężenie-odkształcenie dla stali węglowej w podwyższonych temperaturach [147]

Fig. 2.6. The stress-strain relation of carbon steel in elevated temperature range

The diagrams with regard to S235 steel at various temperatures

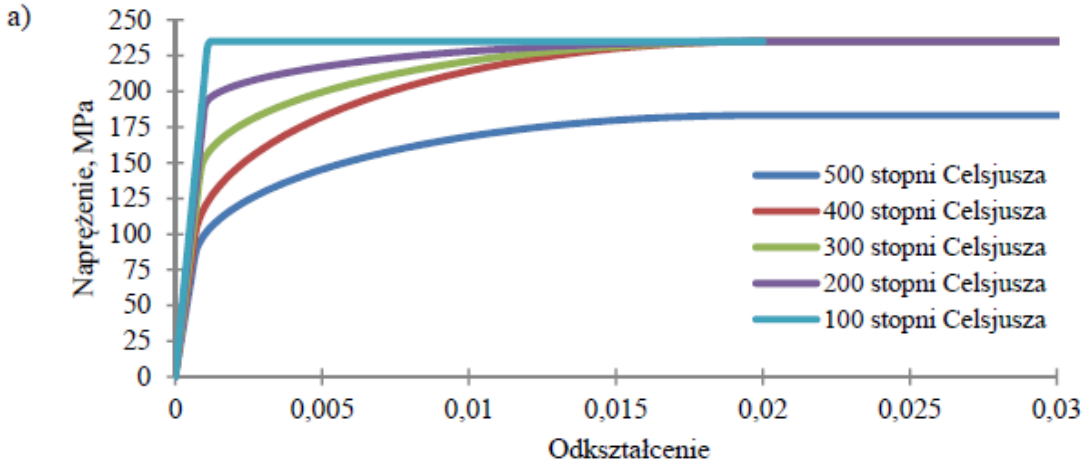

Fig. 2.9. Distinction of fire protection means

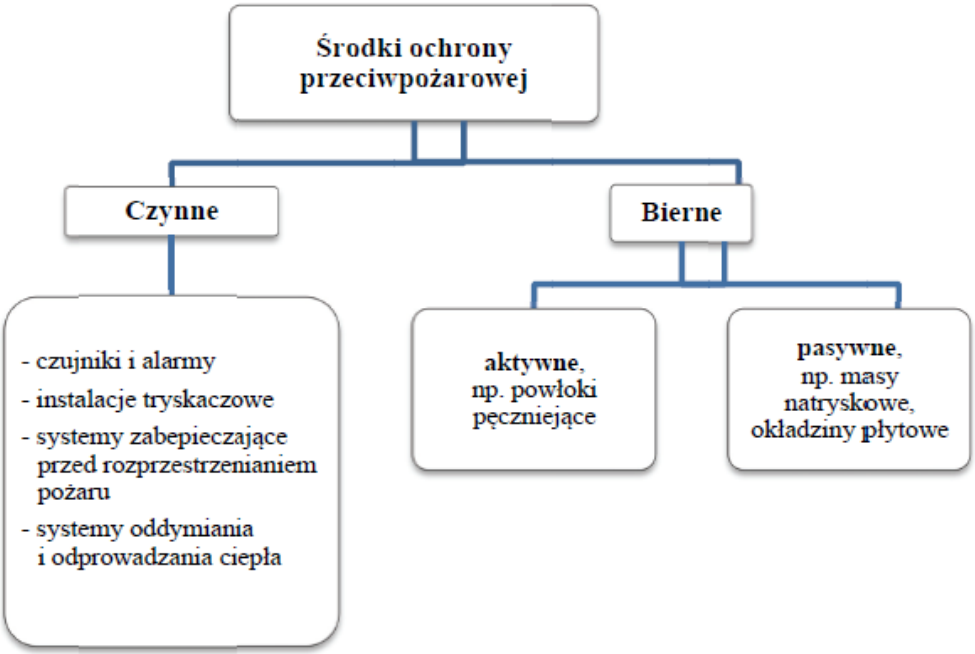

***Rys. 2.9.** Podział środków ochrony pożarowej*

the means of fire protection active - sensors and alarms – sprinklers - fire-retarding systems - smoke and heat discharging systems passive active-type, e.g. expanding coatings passive-type, e.g. spray-on layers, plate tiles

The methods of fire analysis

five phases may be distinguished in the fire course

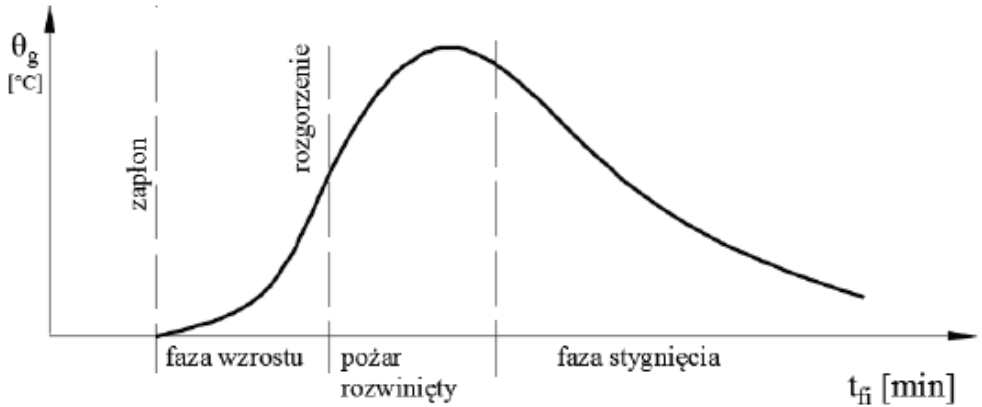

Rys. 2.10. Fazy pożaru

Fig. 2.10 Fire phases ignition flashover growth developed fire decay (cooling)

Structural design in an extraordinary case, based on thermal reaction analysis upon a standard fire

The rise of fir gas temperature θ_g makes the temperature of steel element θ_a rise, its resistance *N* decreases.

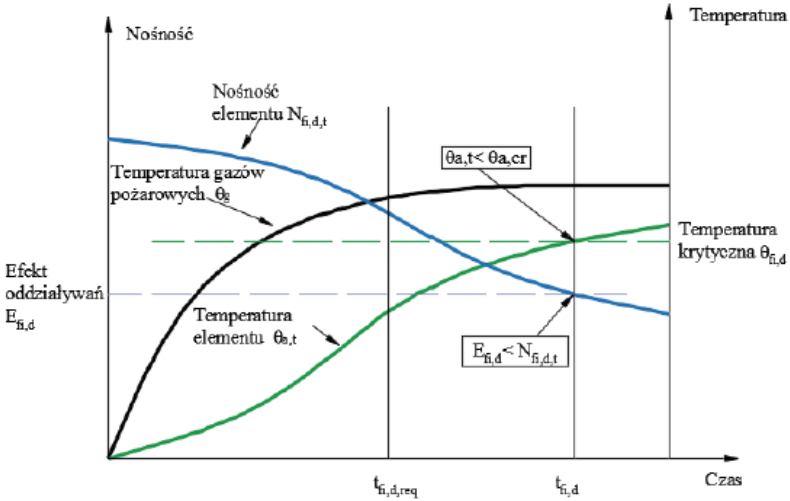

***Rys. 2.11.** Metody analizy pożarowej [73]*

The fire-oriented design specifies one out of the following two conditions fulfilled in a specified $t_{fi,req}$ time:

$\theta_{cr} \geq \theta_a$ – check in temperature domain,

$\theta_{cr} \geq \theta_a$ – check in resistance domain.

Fire diagrams (curves)

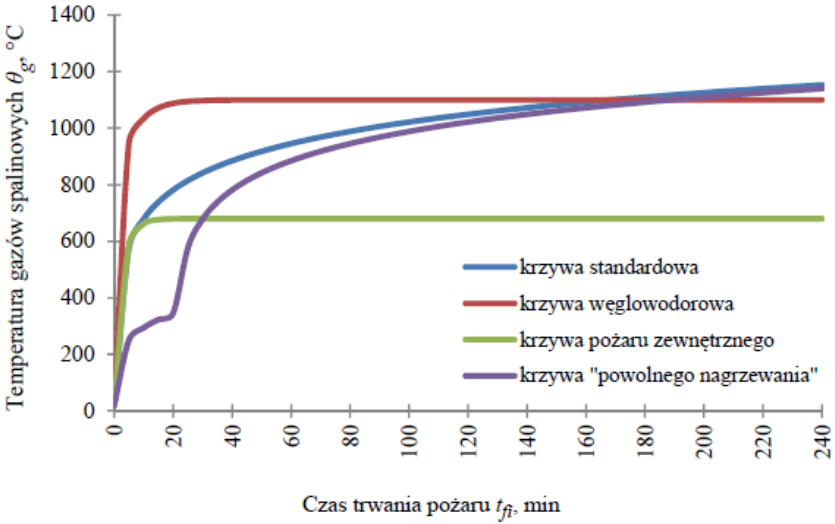

***Rys. 2.12.** Nominalne krzywe pożarowe temperatura-czas*

Fig. 2.12. Nominal temperature-time fire diagrams

standard curve, hydrocarbon curve, external fire curve,
the curve of „slow heating”

Design (dimensioning) of truss structural elements due to fire conditions.

Elements at tension

Design resistance of an element at tension, of a uniform temperature is stated by the formula

$$N_{fi,\theta,Rd} = k_{y,\theta_a} N_{Rd} [\gamma_{M,0} / \gamma_{M,fi}] \qquad (2.55)$$

where

N_{Rd} – design cross-sectional resistance, equal $N_{pl,Rd}$ in standard temperature,

k_{y,θ_a} - reduction factor for yield stress in an element temperature θ produced by fire t_{fi}, according to table 2.5

$\gamma_{M,0}$ - partial factor applied in the cross-sectional resistance check

$\gamma_{M,fi}$ - partial factor concerning material parameters in fire situation

The factors $\gamma_{M,0}$ and $\gamma_{M,fi}$ are equal to 1.0.

Elements at compression

The elements at compression of 1, 2 or 3 cross-sectional classes and uniform element temperature θ_a show the design buckling resistance in fire duration t_{fi} stated by the formula

$$N_{fi,\theta,Rd} = \chi_{fi} A k_{y,\theta_a} f_y / \gamma_{M,fi} \qquad (2.56)$$

$\gamma_{M,fi}$ - partial factor concerning material parameters in fire situation

k_{y,θ_a} - reduction factor for yield stress in an element temperature produced by fire, according to table 2.5

A - cross-sectional area

f_y - yield stress

$\gamma_{M,fi}$ - flexural buckling factor in a design fire situation, according to the formula

$$\chi_{fi} = \frac{1}{\varphi_{\theta_a} + \sqrt{\varphi_{\theta_a}^2 - \overline{\lambda}_{\theta_a}^2}} \qquad (2.57)$$

while
- relative slenderness in a basic design situation
- reduction factor for yield stress and linear elasticity modulus, respectively, for steel in a temperature equal according to the Tab. 2.5.

przy czym

$$\varphi_{\theta_a} = \frac{1}{2}\left[1 + \alpha\overline{\lambda_{\theta_a}} + \overline{\lambda_{\theta_a}}^2\right] \tag{2.58}$$

oraz

$$\alpha = 0,65\sqrt{235 / f_y} \tag{2.59}$$

Smukłość względna $\overline{\lambda_\theta}$ w temperaturze θ_a jest określona wzorem:

$$\overline{\lambda_{\theta_a}} = \overline{\lambda}\left[k_{y,\theta_a} / k_{Y,\theta_a}\right]^{0,5} \tag{2.60}$$

gdzie:

$\overline{\lambda}$ – smukłość względna w podstawowej sytuacji projektowej,

k_{y,θ_a}, k_{Y,θ_a} – odpowiednio współczynnik redukcyjny granicy plastyczności i modułu sprężystości liniowej stali w temperaturze θ_a, określone zgodnie z tabelą 2.5.

FIRE-ORIENTED STRUCTURAL DESIGN REGARDING PROBABILISTIC METHODS

Failure probability is a measure of structural safety (p_f).
It is inconvenient to deal with failure probability directly, so reliability index is often incorporated instead (β).
The transformation between two measures is made possible by the use of standard Gauusian CDF, the so-called Laplace function (Φ):

$$\beta = -\Phi^{-1}(p_f) \tag{2.61}$$

$$p_f = -\Phi(-\beta) \tag{2.62}$$

Tabela 2.12. Minimalne wskaźniki niezawodności

Klasy niezawodności	Minimalne wartości β	
	Okres odniesienia 1 rok	Okres odniesienia 50 lat
RC3	5,2	4,3
RC2	4,7	3,8
RC1	4,2	3,3

Tab. 2.12 Minimum reliability indices
reliability classes minimum beta values
reference period – 1 year reference period – 50 years

Tabela 3.1. *Zależność między prawdopodobieństwem awarii a wskaźnikiem niezawodności*

p_f	10^{-1}	10^{-2}	10^{-3}	10^{-4}	10^{-5}	10^{-6}	10^{-7}
β	1,28	2,32	3,09	3,72	4,27	4,75	5,20

Tab. 3.1. Relation between failure probability and reliability index

Failure probability of a structue in fire conditions is defined as follows

$$p_f = P(E \geq N) \tag{2.63}$$

where E – load effect,
N – resistance (load-carrying capacity)

$$p_f = P(E \geq N) \tag{2.63}$$

In the case of fire the probability expressed by (2.63) is usually considered conditional probability, the condition here is a fire event.
Thus (2.63) may be presented in a form:

$$p_f = P\left(\mathit{failure} / \mathit{fire}\right) = P\left(\mathit{fire} \cap \mathit{failure}\right) / P\left(\mathit{fire}\right) \tag{2.64}$$

The probability P(fire) is expressed by

$$P\left(\mathit{fire}\right) = p^{\mathit{ignition}}\, p_f^{\mathit{extinguishing}} = p^{\mathit{ignition}} \left(p_f^{\mathit{occupants}}\, p_f^{\mathit{sprinklers}}\, p_f^{\mathit{fire\_brigade}} \right) \tag{2.65}$$

The real probabilities should be estimated experimentally, but for the sake of this work they were assessed:

$p_f^{occupants} = 0.40$ and $p_f^{sprinklers} = 0.02,$ $p_f^{fire\_brigade} = 0.10.$

The ignition probability is usually referred to a specified time period, regarding a single year it may be stated $p_{1\,year}^{ignition} = 10 \cdot 10^{-6}$

Considering the fire-covered area equal $A_f = 40$ m^2, ignition probability referred to the 50-year period equals

$$p_{50\,years}^{ignition} = 10 \cdot 10^{-6} \cdot 50 \cdot 40 = 0.02 \tag{2.66}$$

This assumption leads to $P(fire)$, according to (2.65) equal:

in the presence of sprinkle installation,

$$P(fire) = 0.02 \cdot 0.4 \cdot 0.02 \cdot 0.1 = 1.6 \cdot 10^{-5} \tag{2.67}$$

in the absence of sprinkle installation

$$P(fire) = 0.02 \cdot 0.4 \cdot 1.0 \cdot 0.1 = 8 \cdot 10^{-4} \tag{2.68}$$

Assuming the probability $P(\ fire\ \cap\ failure)$ equal its maximum allowable value, i.e.

$$P(\ fire\ \cap\ failure) = p_{f,ult} = 7.23 \cdot 10^{-5} \tag{2.69}$$

here the value of $7.23 \cdot 10^{-5}$ corresponds to the reliability index equal 3.8 in a basic design situation, according to (2.64) conditional probability p_f may be computed as follows:

- the presence of sprinkle installation $P(\ fire\ ) = 1.6 \cdot 10^{-5}$

$$p_{f,ult} = \frac{7.23 \cdot 10^{-5}}{1.6 \cdot 10^{-5}} = 4.52 > 1 \tag{2.70}$$

- the absence of sprinkle installation $P(\ fire\ ) = 1.6 \cdot 10^{-5}$

$$p_{f,ult} = \frac{7.23 \cdot 10^{-5}}{8 \cdot 10^{-4}} = 0.0904 \tag{2.71}$$

The fire probability, according to (2.67) is so remote that the computational overall structural safety condition always holds.
Thus further on the second variant is regarded only.

Given p_f, considered a conditional failure probability, the required reliability index in fire conditions may be computed as follows:

$$\beta_{req}^{fire} = -\Phi^{-1}(p_f) = -\Phi^{-1}\left(\frac{P(fire \cap failure)}{P(fire)}\right) \cong 1.34 \qquad (2.72)$$

In the further part this value will serve as the reference, the lowest required for the structure.

System analysis

Decisive (critical) elements are components of the load-carrying system, losing their ability to carry loads due to external loading increment, subsequently, turning the structural system into a mechanism (kinematically variable system, kinematic chain).

System analysis groups the decisive elements into **minimum critical sets (in Polish - MKZ)**, yielding the system effective upon the condition of one element of the set effective only.

These sets are associated with the **kinematically allowable failure mechanisms (in Polish - KDMZ)**, allowing to define reliability structure of a load-carrying structural system. The basic reliability structures will be presented in detail further on.

The definition of KDMZs is the most challenging part of system reliability analysis, to be possibly solved by a couple of methods, e.g. the method of „elastic solutions”, the method of moment equalization and by linear programming methods.

The task is completed here by means of spectral analysis of a linear stiffness matrix.

In order to complete the task a linear eigenvalue problem is solved:

$$\left(\mathbf{K}_L - \lambda \mathbf{I}\right)\mathbf{q} = \mathbf{0}$$

where
$\mathbf{K}_L$ – linear stiffness matrix,
$\mathbf{q}$ – deflection vector,
λ – eigenvalues of a linear stiffness matrix.

Eigenvalues λ of a linear stiffness matrix denote energetic states of a structural model, the eigenvectors represent the form of principal strains.

While the eigenvalues are positive, the structure is geometrically stable.

The presence of zero eigenvalues is equivalent to turning a structure into a mechanism.

Identification of possible mechanisms is performed by means of a FEM-based software in Mathematica environment.

Series structural systems

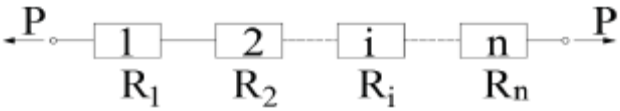

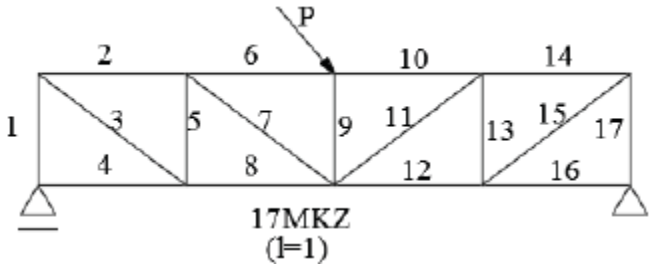

Reliability of a static model following the series pattern is assessed by the formula:

$$R = \prod_{i=1}^{n} R_i = R_1 R_2 .... R_n$$

here *n* is a number of decisive elements of the considered system, the work specifies n a number of elements in the truss

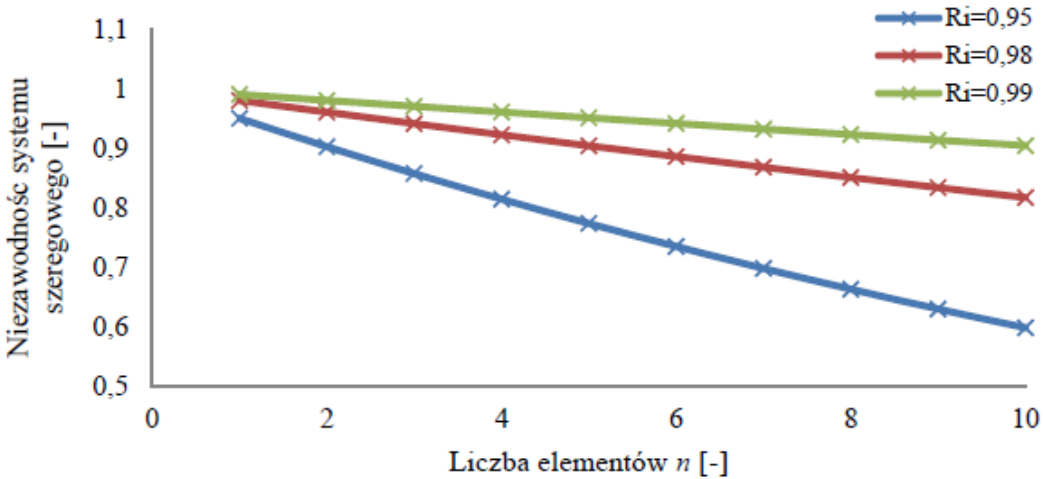

***Rys. 3.11.** Zależność wskaźnika niezawodności systemu szeregowego od liczby elementów*

Fig. 3.11. Relation of a series system reliability vs the number of elements
the number of elements reliability of a series system

Fig. 3.11 plainly shows a recognized effect of statistical structural weakening of a series structural system, showing a rapid reliability decrement with the rise of a number of elements.

Parallel structural systems

A parallel model is appropriate for selected statically indeterminate structures.

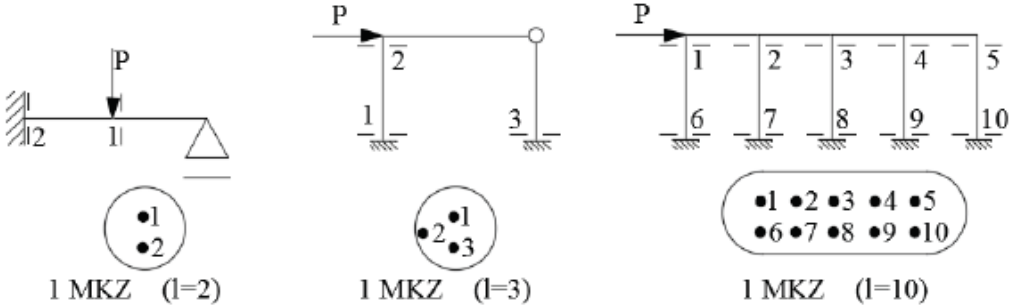

Rys. 3.13. Przykłady schematów konstrukcji o równoległym modelu niezawodnościowym [10]

Fig. 3.13 Structural examples of a parallel reliability model

Reliability of a parallel system may bye computed by a formula:

$$R = 1 - \prod_{i=1}^{n} (1 - R_i)$$

In general, increment of elements in a parallel connection rises overall system reliability. However, a large number of connected elements, common in civil engineering, makes the strengthening effect slow down.

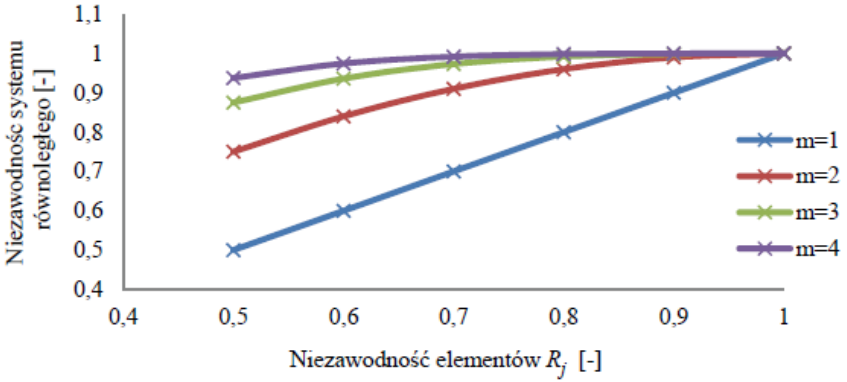

Rys. 3.14. *Zależność wskaźnika niezawodności systemu równoległego od liczby elementów w funkcji niezawodności pojedynczego elementu*

Fig. 3.14 Reliability index of a parallel system related to the number of elements in the function of a single element reliability

Structural design makes it essential to note that series element connections (statically determinate structures) show a substantial reliability decrease, while parallel connections (statically indeterminate structures) bring about a slight reliability rise only.

The majority of statically indeterminate structures corresponds to a **mixed system model**.

Parallel-series and series-parallel are two basic mixed system patterns. However, the real mixed systems are usually more complex.

The further work assumes separation of minimum critical sets (MKZs)

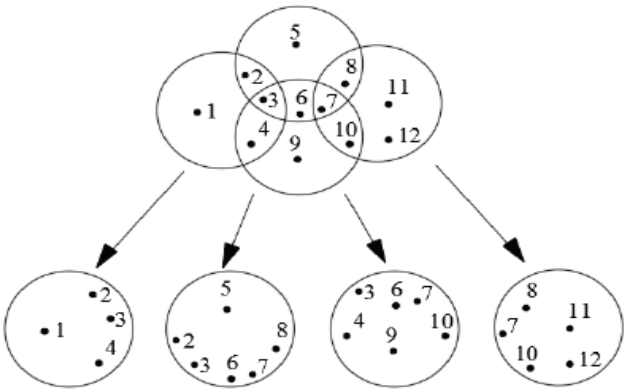

Rys. 3.15. Rozseparowanie minimalnych krytycznych zbiorów konstrukcji o mieszanym modelu niezawodnościowym z elementami wspólnymi [10]

Fig. 3.15 Separation of minimum critical structural sets (MKZ) of a mixed reliability model, including common elements

A plane truss analysed by means of standard curve and „exponential” curve

Standard curve and „exponential” curve:

$$\theta_g = 345 \log_{10}(8t_{fi} + 1) + 20$$

$$\theta_g = 20 \cdot e^{0{,}08465 \cdot t_{fi}}$$

where

θ_g - temperature of fire gases,

t_{fi} - fire duration, minutes

Rys. 4.2. Krzywa standardowa i krzywa "wykładnicza"

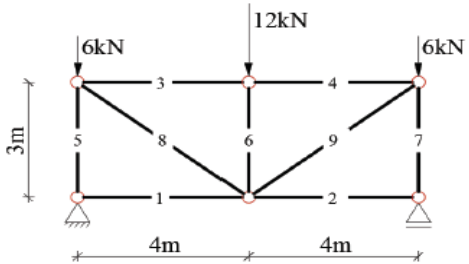

Rys. 4.1. *Schemat statyczny i obciążenie analizowanej kratownicy*

Fig. 4.1. Static model and loading of the analysed truss

Tabela 4.1. *Profile, efekty oddziaływań i nośności poszczególnych elementów kratownicy*

Element	1	2	3	4	5	6	7	8	9
Profil	I 80		I 100		RO 44.5x5			RO 20x2.3	
Efekt oddziaływań, kN	0		-8		-12			10	
Nośność w chwili $t = 0$, kN	5		14,64		25,92			35,2	

Tab. 4.1. Profiles, load effects and resistances of distinct truss members

Element, profile, load effect, kN, resistance at the instant t = 0

The presented example conducts temperature analysis of insulated and uninsulated members.
The fireproof coating was a spray-on layer of 1.5 cm thick mineral fibre whose parameters are: density, specific heat, heat conductivity.
The analytical results are presented in Figs. 4.4 – 4.7.
The dotted line marks fire curves, the solid line denoted temperature of steel members.

a)

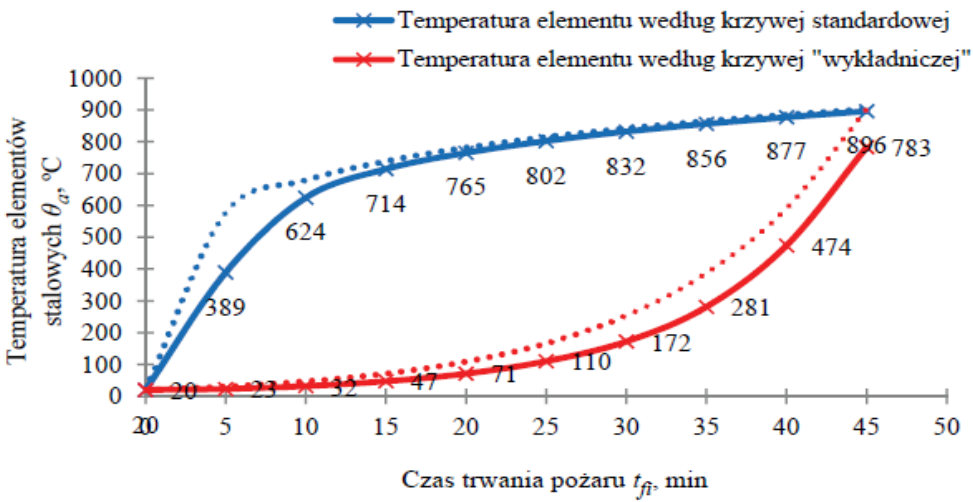

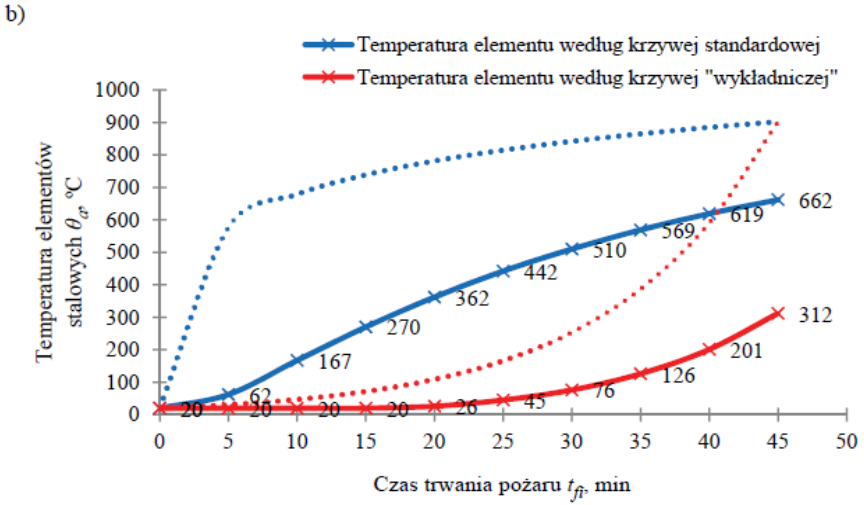

Rys. 4.4. Temperatura nieizolowanych (a) i izolowanych (b) elementów pasa dolnego (elementy 1, 2) przy zastosowaniu różnych krzywych pożarowych

Fig. 4.4. Temperature of insulated (a) and uninsulated (b) lower chord members (no. 1 and 2) applying various fire curves

element temperature according to standard curve / „exponential" curve
temperature of steel elementsfire duration

The presented example proves that fire curve characteristic is decisive to the thermal structural response

Tabela 4.4. Spadek modułu sprężystości i granicy plastyczności w czasie rozwoju pożaru

Czas trwania pożaru t_{fi}, min	Standardowa krzywa pożarowa		Węglowodorowa krzywa pożarowa		Krzywa pożaru zewnętrznego	
	Moduł sprężystości Y, GPa	Granica plastyczności f_y, MPa	Moduł sprężystości Y, GPa	Granica plastyczności f_y, MPa	Moduł sprężystości Y, GPa	Granica plastyczności f_y, MPa
0	210	235	210	235	210	235
5	210	235	210	235	210	235
10	210	235	200	235	210	235
15	210	235	188	235	202	235
20	207	235	177	235	195	235
25	199	235	166	235	189	235
30	191	235	157	235	183	235
35	183	235	148	235	177	235
40	176	235	140	218	172	235
45	169	235	133	200	167	235
50	162	235	125	182	163	235
55	155	235	101	160	158	235
60	149	235	89	140	154	235

Tab. 4.4. The decrement of elasticity modulus and yield stress in the fire course

fire duration, standard fire curve, hydrocarbon fire curve, the curve of external fire, elasticity modulus, yield stress

THE IMPACT OF THERMAL INSULATION TYPE AND THICKNESS ON MECHANICAL RESPONSE OF A STRUCTURE IN FIRE CONDITIONS

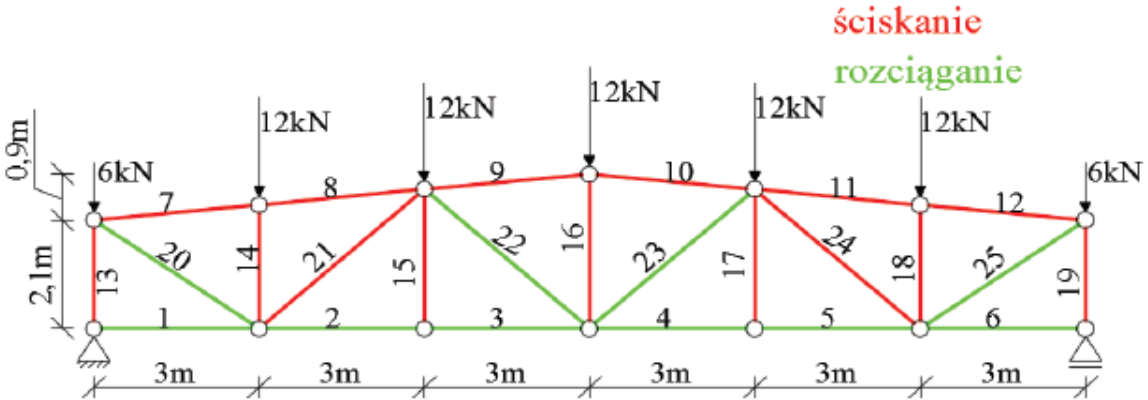

Rys. 4.11. *Schemat statyczny analizowanej kratownicy*

Fig. 4.11 Static model of the analysed truss

Tabela 4.5. Przekroje elementów kratownicy i efekty oddziaływań

	Profil	Efekt oddziaływań
Pas dolny	I 100	$N_1 = N_6 = 0$ kN $N_2 = N_3 = N_4 = N_5 = 53{,}33$ kN
Pas górny	IPE 140	$N_7 = N_8 = N_{11} = N_{12} = -37{,}69$ kN $N_9 = N_{10} = -54{,}27$ kN
Skratowanie	RK50x50x5	$N_{13} = N_{19} = -36$ kN $N_{14} = N_{16} = N_{18} = -12$ kN $N_{15} = N_{17} = 0$ kN $N_{20} = N_{25} = 45{,}77$ kN $N_{21} = N_{24} = -21{,}30$ kN $N_{22} = N_{23} = 0{,}90$ kN

Tab. 4.5. Cross-sections of truss elements and load effects

Profile load effect lower chord upper chord diagonals and verticals

Fire analysis of a truss was conducted using four different insulation types.

The first analytical phase assumed the insulation thickness equal 2 cm.

The following insulation types were considered:

- fireproof vermiculite mortar
- fireproof vermiculite-gypsum mortat of higher density
- contour insulation made of cement-vermiculite plate,
- box-shaped insulation made of cement-vermiculite plate

According to formulas (2.52) and (2.53) temperature rise in steel elements is affected by the exposure indicator, among other means.
In the case of spray-on and contour insulations this indicator is equal to the perimeter / cross-sectional area ratio.
In the box-shaped insulation case it equals:

$$\frac{A_p}{V} = \frac{2(b+h)}{A} \tag{4.3}$$

where:
b - cross-sectional width
h - depth
A - area

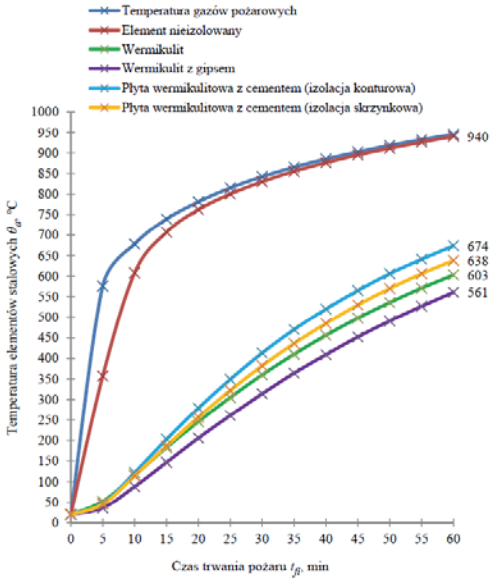

***Rys. 4.12.** Temperatura stalowych elementów pasa dolnego (I 100) przy zastosowaniu różnego typu izolacji o grubości 2 cm*

Fig. 4.12. Temperature of lower chord steel members (I100) applying various 2 cm thick insulation types

temperature of fire gases, uninsulated elements, vermiculite, vermiculite and gypsum, vermiculite plate with cement (contour insulation), vermiculite plate with cement (box-shaped insulation) temperature of steel elements, fire duration

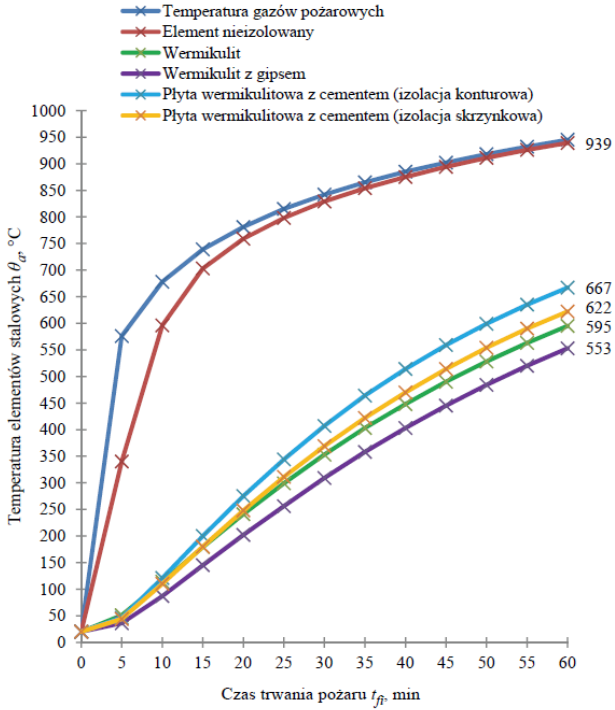

Rys. 4.13. *Temperatura stalowych elementów pasa górnego (IPE 140) przy zastosowaniu różnego typu izolacji o grubości 2 cm*

Fig. 4.13. Temperature of upper chord steel members (IPE 140) applying various 2 cm thick insulation types

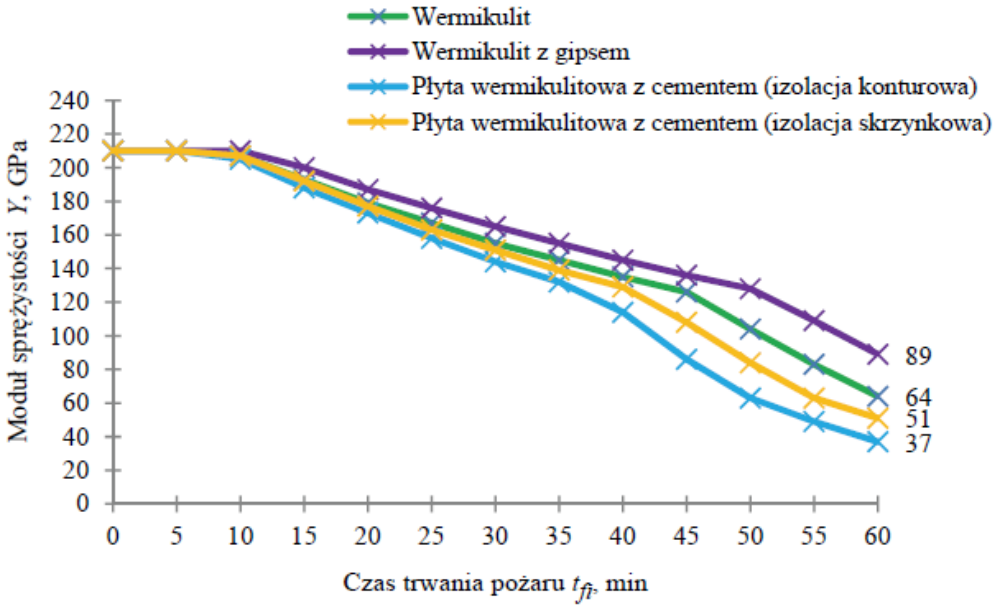

Rys. 4.15. *Zmiana modułu sprężystości elementów pasa dolnego (I 100) wraz z rozwojem pożaru przy zastosowaniu różnego typu izolacji o grubości 2 cm*

Fig. 4.15 Elasticity modulus variation of lower chord elements (I100) due to fire development applying various 2 cm thick insulation types

modulus of elasticity, fire duration

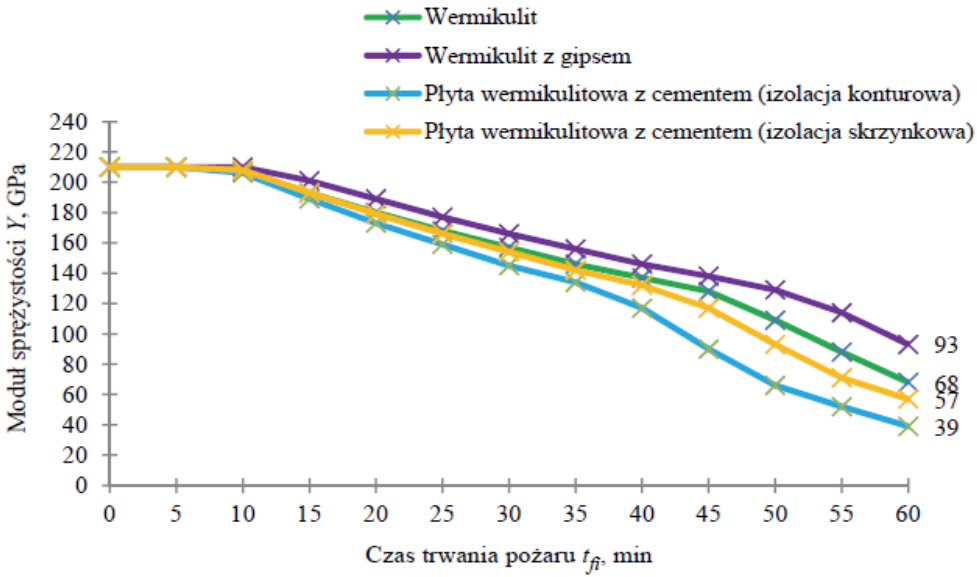

Rys. 4.16. *Zmiana modułu sprężystości elementów pasa górnego (IPE 140) wraz z rozwojem pożaru przy zastosowaniu różnego typu izolacji o grubości 2 cm*

Fig. 4.16 Elasticity modulus variation of upper chord elements (IPE 140) due to fire development applying various 2 cm thick insulation types

modulus of elasticity, fire duration

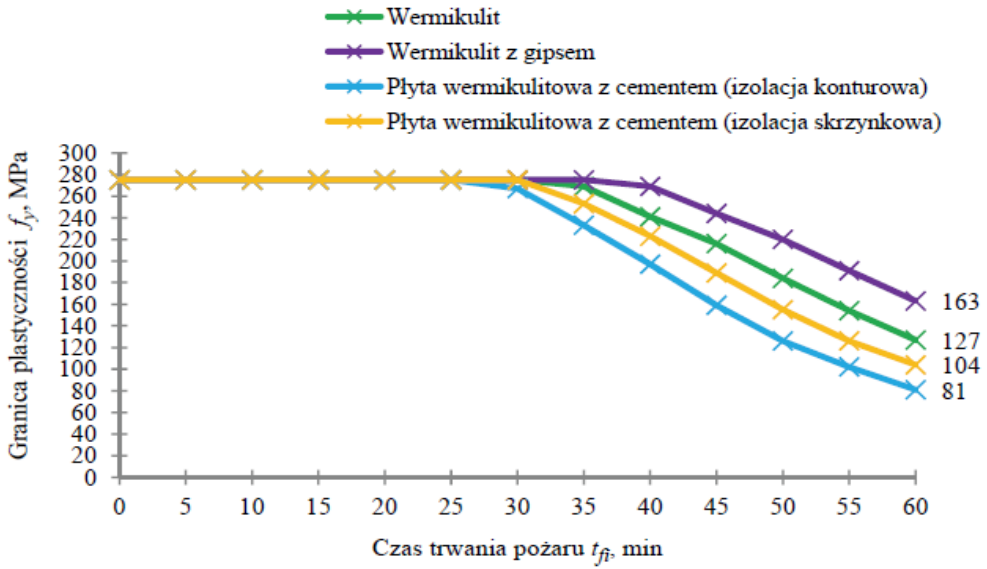

***Rys. 4.18.** Zmiana granicy plastyczności elementów pasa dolnego (I 100) wraz z rozwojem pożaru przy zastosowaniu różnego typu izolacji o grubości 2 cm*

Fig. 4.18 Yield stress variation of lower chord elements (I100) due to fire development applying various 2 cm thick insulation types

yield stress, fire duration

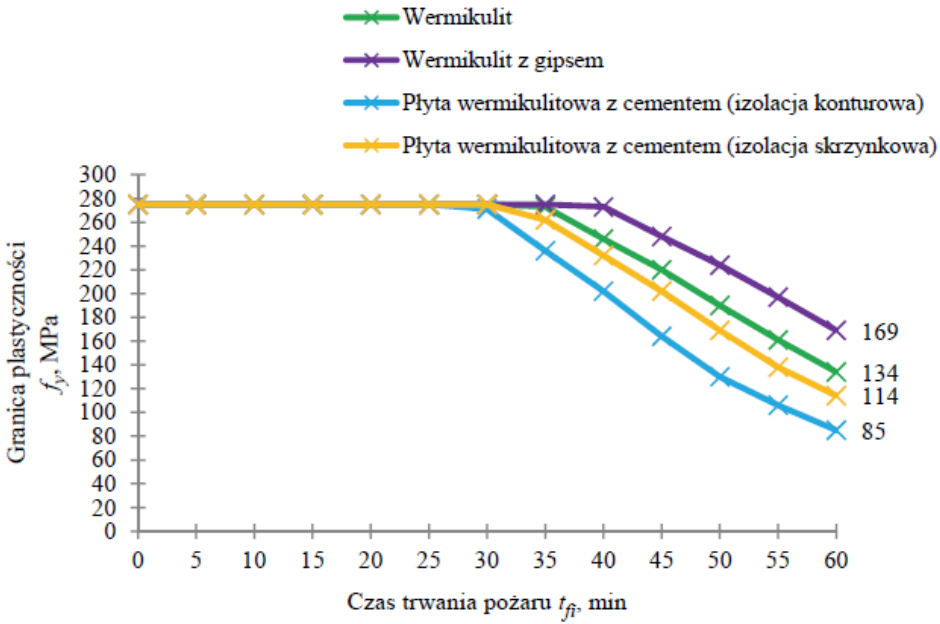

***Rys. 4.19.** Zmiana granicy plastyczności elementów pasa górnego (IPE 140) wraz z rozwojem pożaru przy zastosowaniu różnego typu izolacji o grubości 2 cm*

Fig. 4.19 Yield stress variation of upper chord elements (IPE 140) due to fire development applying various 2 cm thick insulation types

yield stress fire duration

lower chord elements at tension (I 100)

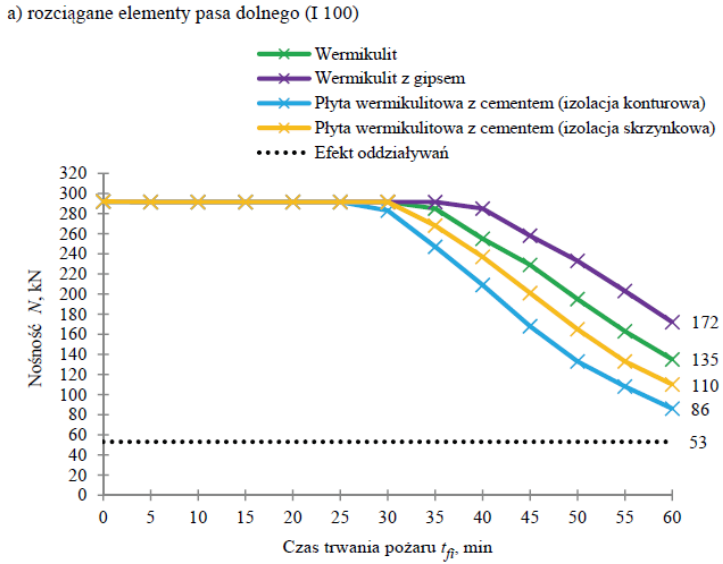

Rys. 4.21. *Spadek nośności elementów kratownicy wraz z rozwojem pożaru przy zastosowaniu różnego typu izolacji o grubości 2 cm*

Fig. 4.21 Resistance decrement of truss elements due to fire evolution, applying various insulation variants of a 2 cm thickness

vermiculite vermiculite and gypsum, vermiculite plate with cement (contour insulation), (box-shaped insulation) load effect

b) upper chord compressed elements (IPE 140

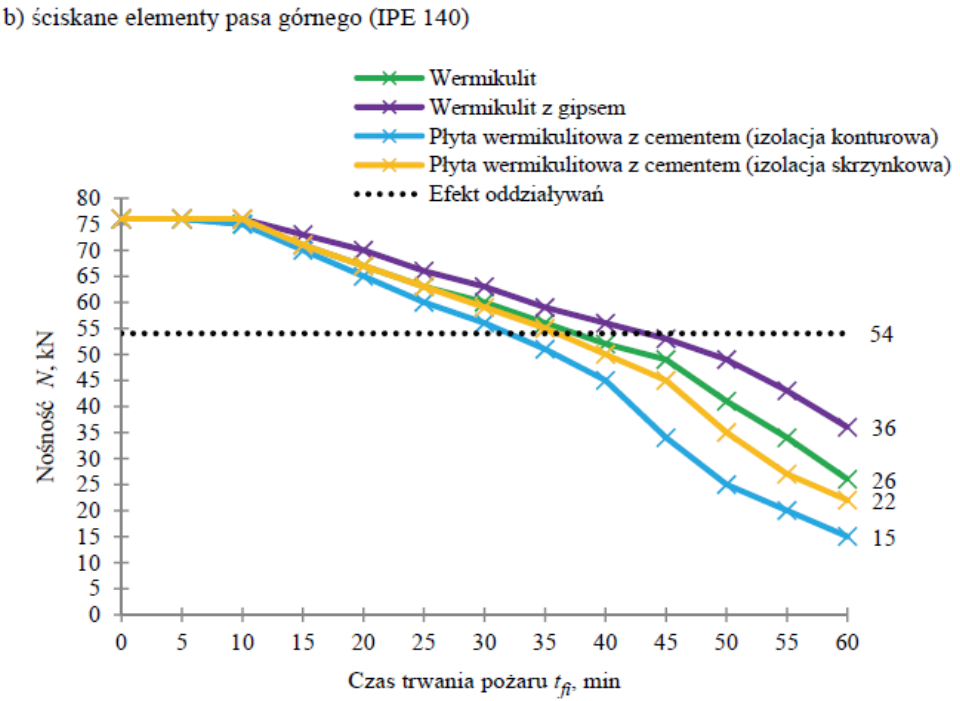

Rys. 4.21. *Spadek nośności elementów kratownicy wraz z rozwojem pożaru przy zastosowaniu różnego typu izolacji o grubości 2 cm*

Fire reliability analysis of a statically determinate plane steel truss

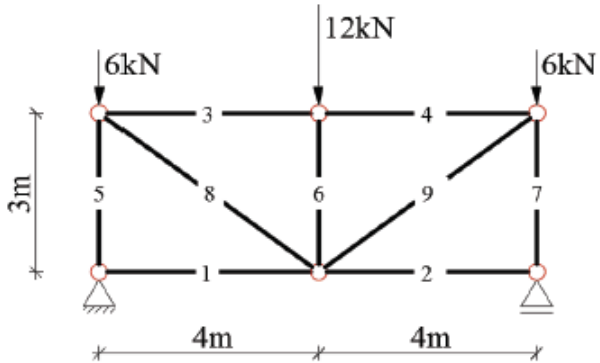

Element	1	2	3	4	5	6	7	8	9
Profil	I 80		I 100		RO 44,5x5			RO 20x2,3	
Efekt oddziaływań, kN	0		-8		-12			10	

Rys. 4.32. Analizowana kratownica statycznie wyznaczalna

Fig. 4.32. The analysed statically determinate truss

element profile load effect

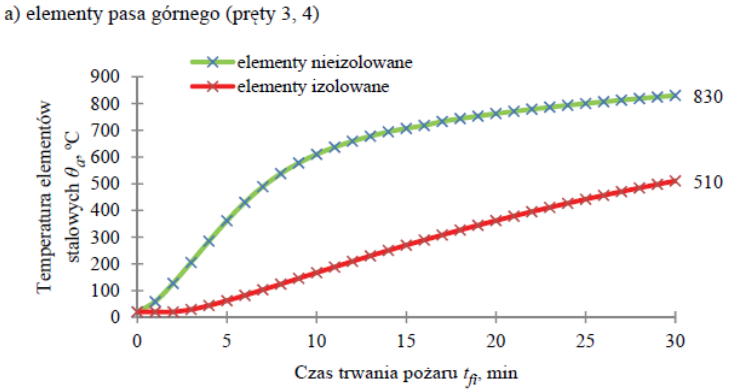

upper chord elements, insulated elements, non-insulated elements, temperature of steel elements, fire duration

The reliability analysis was conducted in the following time periods of fire duration: 0, 5, 10, 15, 20, 25, 30 minutes.

The analysed truss is statically determinate, thus failure of a single element out of the set (1-9) results in overall structural failure.

Thus system reliability (***R***) follows the series system pattern, following the formula:

$$R = \prod_{i=1}^{9} R_i = R_1 \cdot R_2 \cdot R_3 \cdot R_4 \cdot R_5 \cdot R_6 \cdot R_7 \cdot R_8 \cdot R_9$$

The random variables assumed in reliability analysis were defined according to Tab. 4.14.
The reliability indices were estimated on the basis of a dedicated MS Excel spreadsheet

Tabela 4.14. *Probabilistyczne charakterystyki zmiennych losowych dla płaskiej kratownicy statycznie wyznaczalnej*

Zmienna losowa	**Wartość oczekiwana**			**Współczynnik zmienności**	**Odchylenie standardowe**			**Typ rozkładu**
Pole przekroju poprzecznego *A*	10,6 cm^2	6,2 cm^2	1,28 cm^2	6%	0,636 cm^2	0,372 cm^2	0,077 cm^2	normalny
Granica plastyczności f_y	275 000 kPa			8%	22 000 kPa			
Efekt oddziaływań *E*	8 kN	10 kN	12 kN	6%	0,48 kN	0,6 kN	0,72 kN	

Tab. 4.14. Probabilistic parameters of basic random variables with regard to a plane statically determinate truss

Random variable Mean value Coefficient of variation Standard deviation Variable type, Cross-sectional area *A*, yield stress f_Y, load effect *E*

The results of system-based reliability assessment are presented in Fig. 4.34. The required reliability index equal 1.34 is stated here.

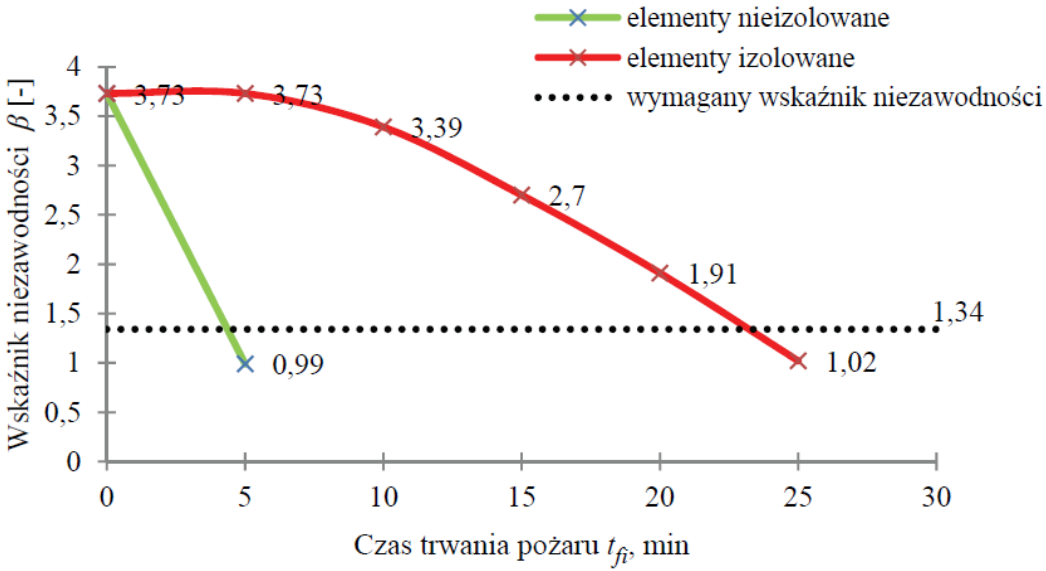

Rys. 4.34. *Monitoring wskaźnika niezawodności płaskiej kratownicy statycznie wyznaczalnej w kolejnych minutach trwania pożaru, uzyskanego przy zastosowaniu metod analizy systemowej*

Tab. 4.15. Reliability indices of a plane, statically determinate truss, various methods of reliability assessment

Tabela 4.15. *Wskaźniki niezawodności dla płaskiej kratownicy statycznie wyznaczalnej uzyskane przy zastosowaniu różnych metod analizy niezawodności*

Czas trwania pożaru t_{fi}, min	Wskaźnik niezawodności β					
	FORM	SORM	Importance Sampling	Monte Carlo	Analiza systemowa	Wskaźnik niezawodności dla elementu
0	4,30	4,30	4,25	4,11	3,73	3,96
5	4,30	4,30	4,25	4,11	3,73	3,96
10	3,86	3,86	3,81	3,72	3,39	3,61
15	3,12	3,12	3,04	3,06	2,70	2,95
20	2,31	2,31	2,25	2,27	1,91	2,22
25	1,47	1,47	1,41	1,48	1,02	1,43
30	0,57	0,56	0,55	0,60	<0	0,56

Fig. 4.36 compares reliability indices regarding to various methods of reliability assessment

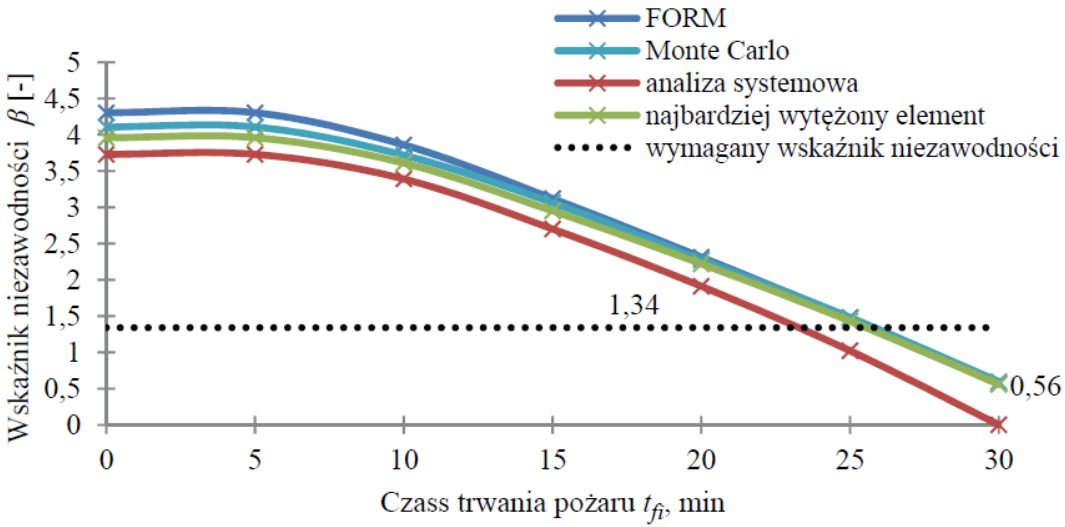

Rys. 4.36. *Monitoring wskaźnika niezawodności obliczonego według różnych metod w kolejnych minutach trwania pożaru*

Fig. 4.36. Reliability index monitoring regarding various methods, subsequent minutes of fire duration

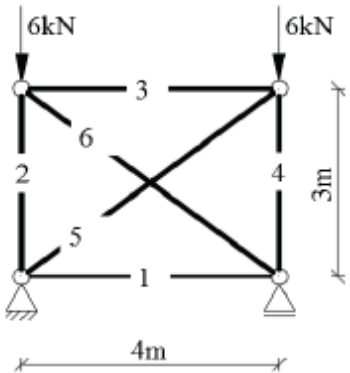

Elementy	1,3	2,4	5,6
Profil (Kratownica "A")	I 80	RO 33,7x3,6	RO 30x3,2
Profil (Kratownica "B")	RO 33,7x4	RO 33,7x4	RO 33,7x4

Rys. 4.39. Kratownica jednokrotnie statycznie niewyznaczalna

Fig. 4.39. A single-degree statically indeterminate truss

Tabela 4.25. Analiza termiczna elementów pasów kratownicy "A"

I80					
Czas trwania pożaru t_{fi}, min	Temperatura elementu θ_a, °C	Moduł Younga Y, GPa	Granica plastyczności f_y, MPa	Nośność elementów rozciąganych, kN	Nośność z uwzględnieniem wyboczenia (elementy ściskane), kN
0	20	210	275	208,18	7,64
5	85,77	210	275	208,18	7,25
10	204,11	188	275	208,18	6,54
15	312,70	165	275	208,18	5,79
20	406,21	146	271	205,33	5,13
25	484,99	129	224	169,25	4,53
30	550,88	95	171	129,54	3,34

Tab. 4.25 Thermal analysis of chord members of the truss

fire duration tf, min member temperature theta a, C Young's modulus, Y, yield stress fY, tensile load-bearing capacity, kN, compressive load-bearing capacity (buckling considered), kN

The reliability viewpoint of the analysed structure points out the mixed (hybrid) system appropriate.
It is required here to define kinematically allowable failure mechanisms (In Polish - KDMZ)
The first mechanism (KDMZ) and its appropriate structural model are presented in Fig. 4.40.

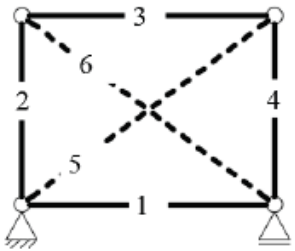

$$R_I = 1 - (1 - R_5)(1 - R_6)$$

Rys. 4.40. *I kinematycznie dopuszczalny mechanizm zniszczenia dla konstrukcji statycznie niewyznaczalnej*

Fig. 4.40. The 1st kinematically allowable mechanism of a statically indeterminate truss

The 2nd kinematically allowable failure mechanism KDMZ (Fig. 4.41) refers to failure of a single diagonal of (5,6) and one of the elements 1-4.
This mechanism requires a two-step reliability assessment: first the series model (*RIIA*, *RIIB*), next, the parallel routine (*RII*)

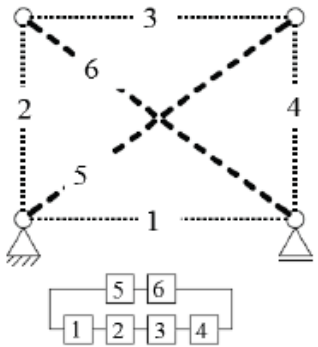

$$R_{IIA} = R_5 \cdot R_6$$

$$R_{IIB} = R_1 \cdot R_2 \cdot R_3 \cdot R_4$$

$$R_{II} = 1 - (1 - R_{IIA})(1 - R_{IIB})$$

Rys. 4.41. *II kinematycznie dopuszczalny mechanizm zniszczenia dla konstrukcji statycznie niewyznaczalnej*

Fig. 4.41. The 2nd kinematically allowable mechanism of a statically indeterminate truss

The 3rd kinematically allowable failure mechanism KDMZ (Fig. 4.42) corresponds to failure of any pair out of the members 1-4.
Reliability of such system is computed in a parallel-series routine, as presented below

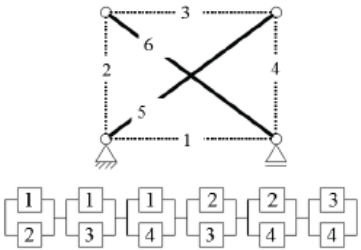

$$R_{IIIA} = 1-(1-R_1)(1-R_2)$$
$$R_{IIIB} = 1-(1-R_1)(1-R_3)$$
$$R_{IIIC} = 1-(1-R_1)(1-R_4)$$
$$R_{IIID} = 1-(1-R_2)(1-R_3)$$
$$R_{IIIE} = 1-(1-R_2)(1-R_4)$$
$$R_{IIIF} = 1-(1-R_3)(1-R_4)$$
$$R_{III} = R_{IIIA} \cdot R_{IIIB} \cdot R_{IIIC} \cdot R_{IIID} \cdot R_{IIIE} \cdot R_{IIIF}$$

Rys. 4.42. *III kinematycznie dopuszczalny mechanizm zniszczenia dla konstrukcji statycznie niewyznaczalnej*

Fig. 4.42 The 3rd kinematically allowable mechanism of a statically indeterminate truss

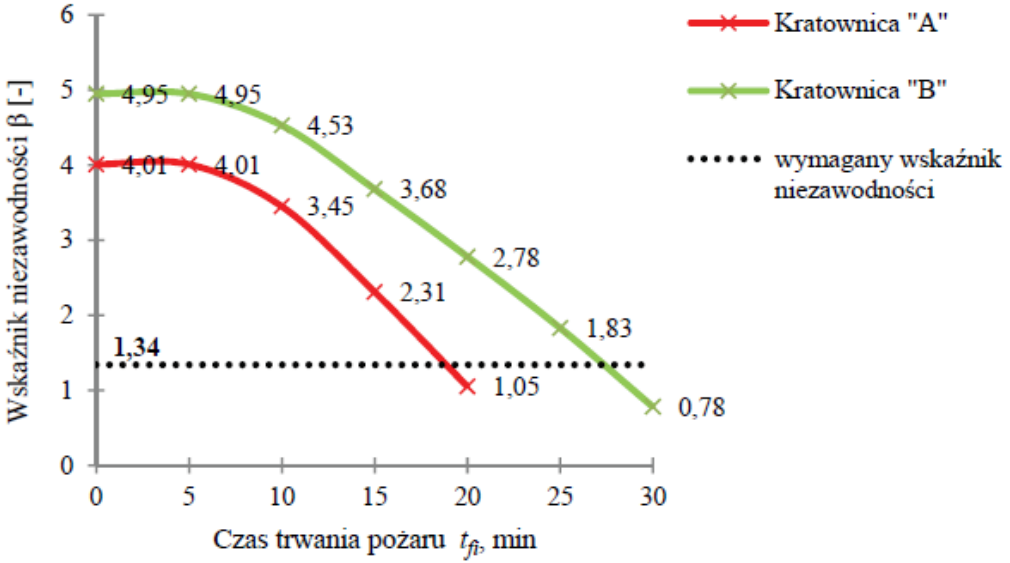

Rys. 4.43. *Monitoring wskaźnika niezawodności kratownicy statycznie niewyznaczalnej w kolejnych minutach trwania pożaru, uzyskanego przy wykorzystaniu analizy systemowej*

Fig. 4.43. Reliability index monitoring of a statically indeterminate truss in subsequent minutes of fire duration, a result of system analysis

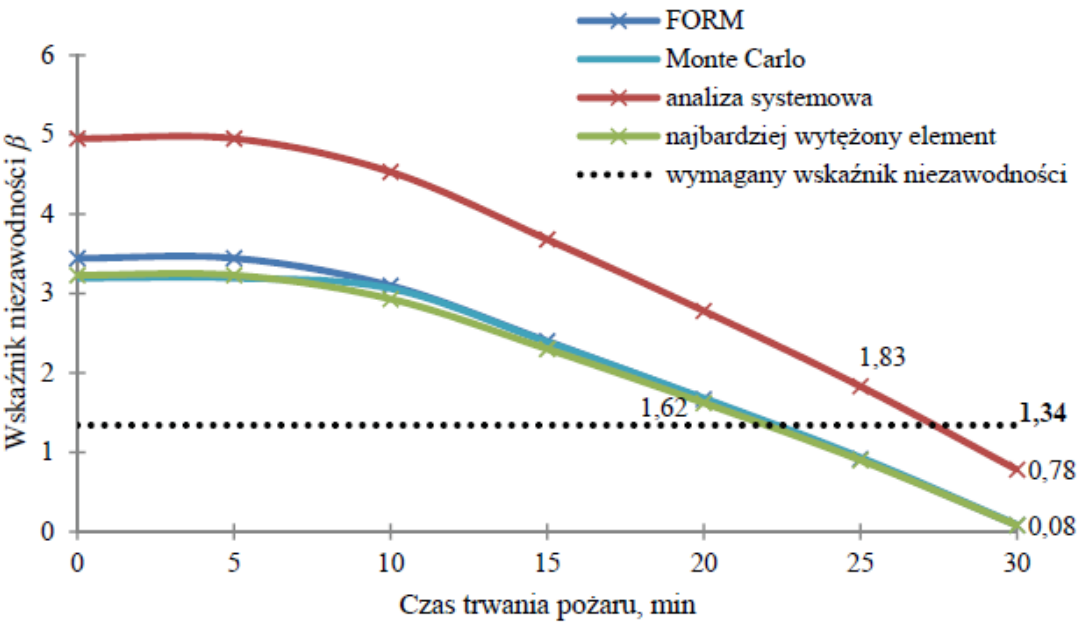

Rys. 4.45. *Monitoring wskaźnika niezawodności uzyskanego według różnych metod dla płaskiej kratownicy jednokrotnie statycznie niewyznaczalnej*

Fig. 4.45. Reliability index monitoring regarding various methods, single-degree of statical indeterminacy

Tab. 4.31. Reliability indices of a plane truss, single-degree of statical indeterminacy

Tabela 4.31. *Wskaźniki niezawodności dla płaskiej kratownicy jednokrotnie statycznie niewyznaczalnej*

Czas trwania pożaru, min	FORM	SORM	Importance Sampling	Monte Carlo	Analiza systemowa	Wskaźnik niezawodności dla elementu
0	3,44	3,44	3,37	3,19	4,95	3,23
5	3,44	3,44	3,37	3,19	4,95	3,23
10	3,10	3,09	3,02	3,06	4,53	2,93
15	2,40	2,40	2,34	2,39	3,68	2,30
20	1,67	1,67	1,63	1,68	2,78	1,62
25	0,92	0,92	0,90	0,94	1,83	0,90
30	0,08	0,08	0,15	0,09	0,78	0,08

System fire reliability analysis – plane steel truss of a multiple degree of statical indeterminacy

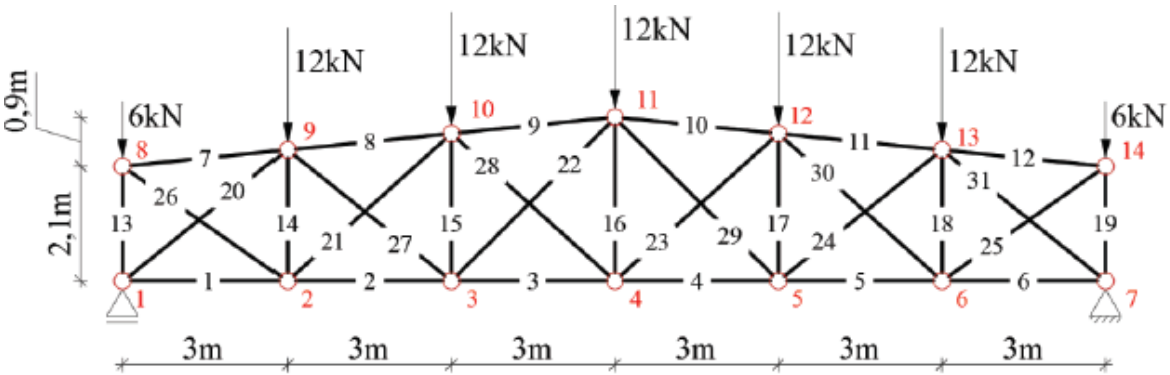

Rys. 4.46. Wielokrotnie statycznie niewyznaczalna kratownica stalowa

Fig 4.46 Steel truss of a multiple degree of statical indeterminacy

The truss is made of S235 steel, its Young's modulus Y = 210 GPa and yield stress f_y = 235 MPa.

The lower chord – HEA100 profile, the upper chord – HEA120 profile, other elements, i.e. diagonals and verticals – square tubes RK 60x60x3.

The structure is insulated by vermiculite-cement mortar, its thickness equals 2 cm, the following parameters: density ρ = 550 kg/m3, thermal conductivity λ_p = 0,12 W/(mK), specific heat c_p = 1100 J/(kgK).

Thermal analysis of the truss has been conducted here.

It covered element temperature, variation of steel parameters (Young's modulus and yield stress) and load-carrying capacity.

The lower chord case is displayed in Tab. 4.34

Tab. 4.34 Thermal analysis of lower chord members of the truss

fire duration tf, min member temperature theta a, C
Young's modulus, Y, yield stress fY,
tensile load-bearing capacity, kN,
compressive load-bearing capacity (buckling considered), kN

Tabela 4.34. Analiza termiczna elementów pasa dolnego

HEA 100					
Czas trwania pożaru t_{fi}, min	**Temperatura elementu θ_a, °C**	**Moduł Younga Y, GPa**	**Granica plastyczności f_y, MPa**	**Nośność elementów rozciąganych, kN**	**Nośność z uwzględnieniem wyboczenia (elementy ściskane), kN**
0	20	210	235	498,2	242,69
5	38,57	210	235	498,2	173,00
10	86,76	210	235	498,2	173,00
15	139,18	201,77	235	498,2	168,65
20	191,09	190,87	235	498,2	162,68
25	241,09	180,37	235	498,2	156,68
30	288,69	170,37	235	498,2	150,76
35	333,67	160,93	235	498,2	144,94
40	375,96	152,05	235	498,2	139,28
45	415,55	143,73	226,96	481,15	132,48
50	452,52	135,97	207,85	440,63	124,15
55	486,96	128,74	190,04	402,89	116,33
60	519,00	114,43	169,46	359,25	103,5

While the truss is statically indeterminate and its members are not uniformly heated with the development of fire, the axial force distribution alters.

The temperature impact increases the forces in the truss members of highest compressive forces, bringing about their buckling failure.

In further fire course the structure still carries the load, but updating its load-carrying model.

a) $t_{fi} = 0$ min

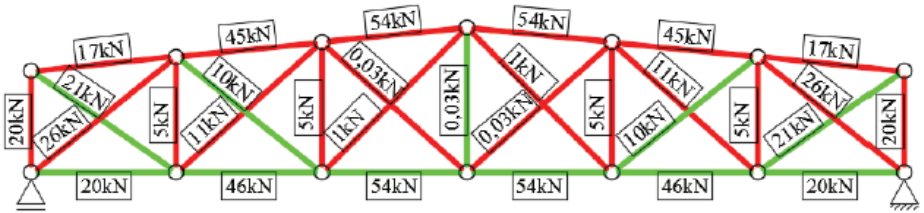

b) $t_{fi} = 5$ min

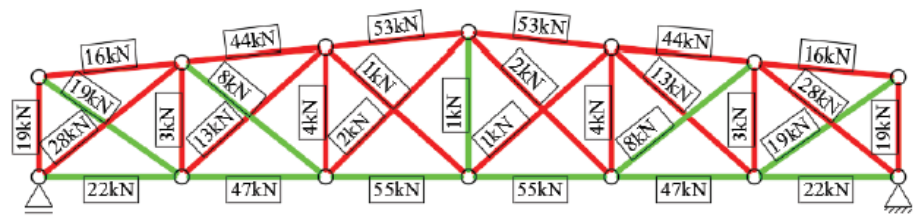

d) t_{fi} = 10,817 min (649 s)

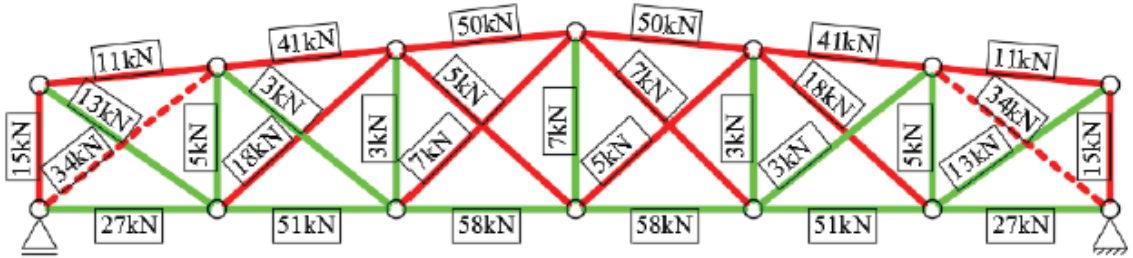

e) t_{fi} = 10,833 min (650 s)

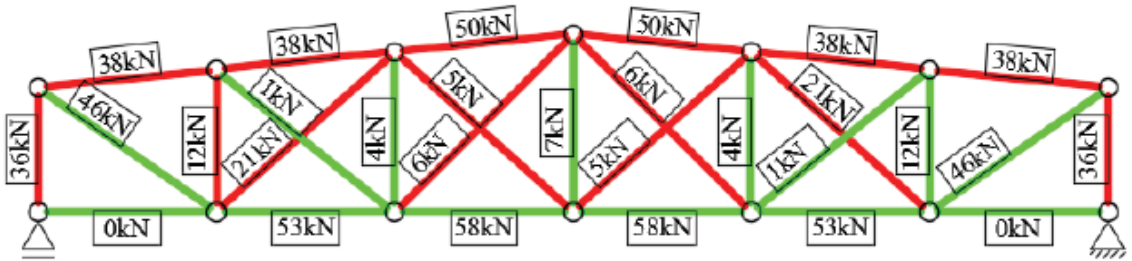

f) t_{fi} = 15 min

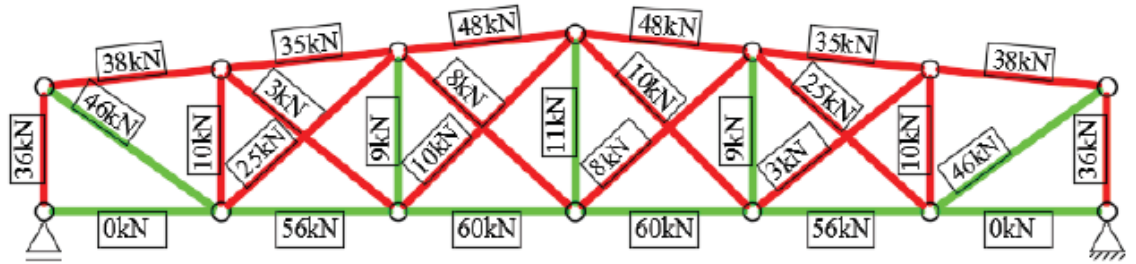

g) t_{fi} = 19,983 min (1199 s)

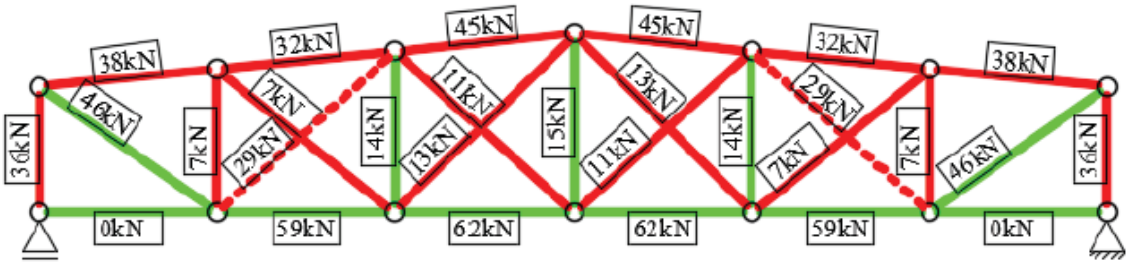

h) t_{fi} = 20 min (1200 s)

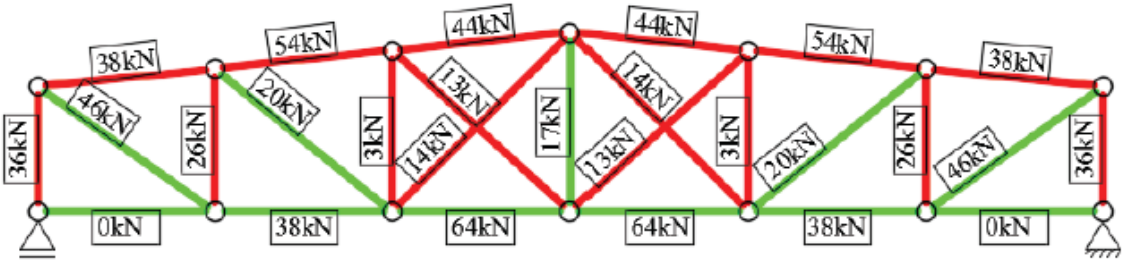

i) t_{fi} = 25 min

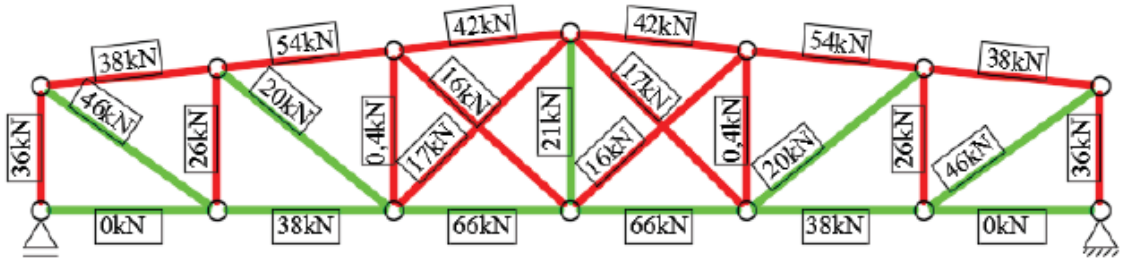

j) t_{fi} = 30 min

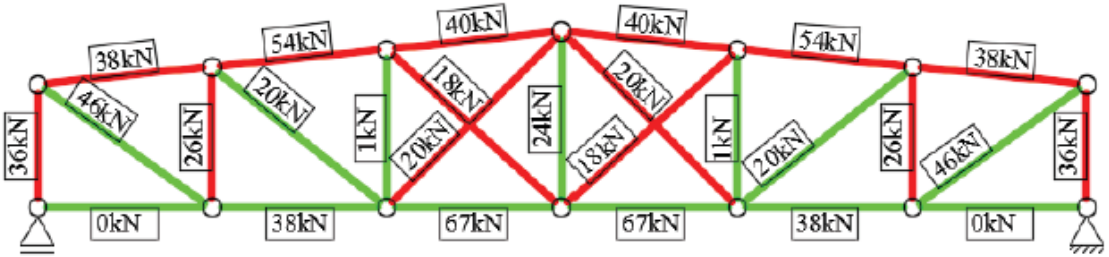

k) t_{fi} = 35 min

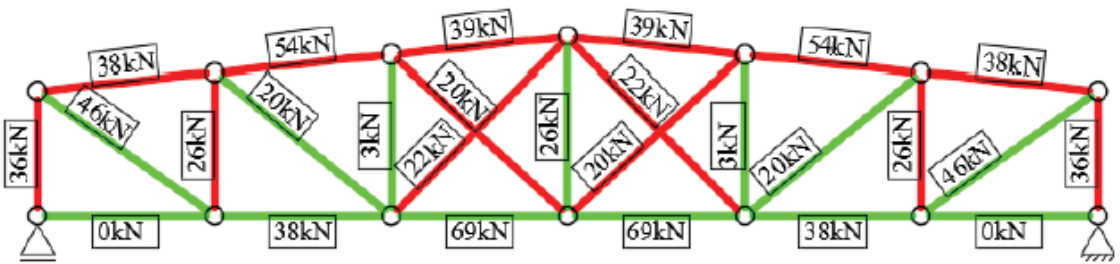

l) t_{fi} = 37,333 min (2240 s)

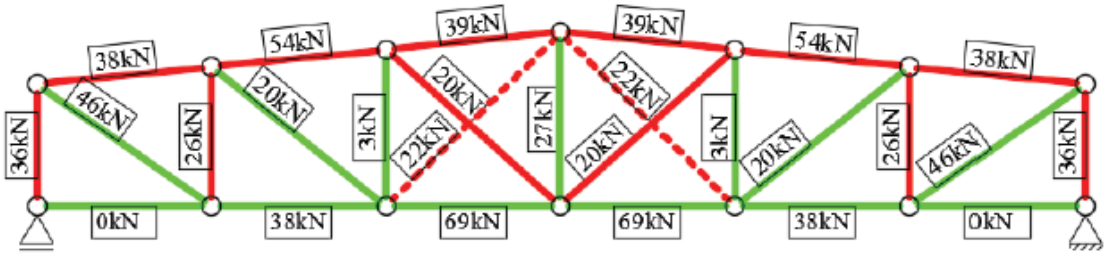

m) t_{fi} = 37,350 min (2241 s) - 59, 717 min (3583 s)

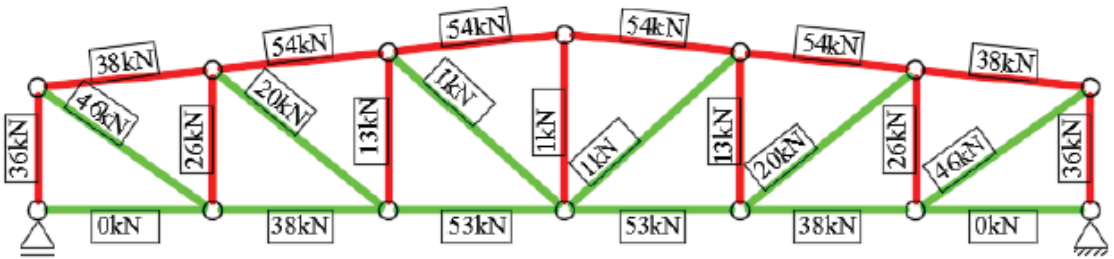

n) t_{fi} = 59,733 min (3584 s)

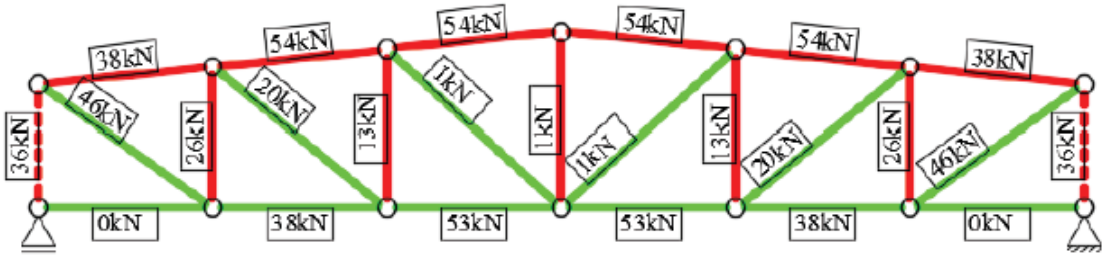

Rys. 4.47. Rozkład sił osiowych w poszczególnych minutach trwania pożaru

4.47 Axial force distribution in selected time instants of fire duration

4.48 Overall truss deflection change in selected time instants of fire duration

4.49 Vertical deflection change of central truss chord nodes in selected time instants of fire duration

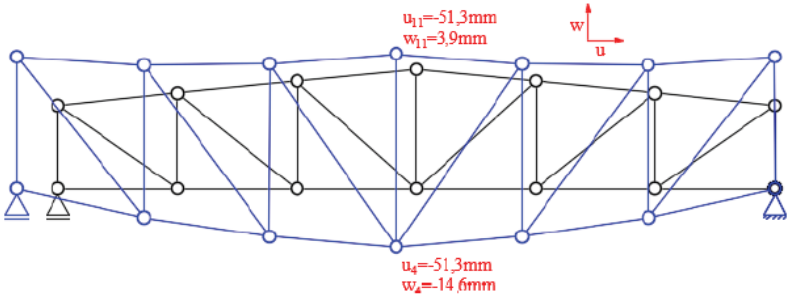

Rys. 4.48. *Zmiana stanu przemieszczeń w poszczególnych minutach trwania pożaru*

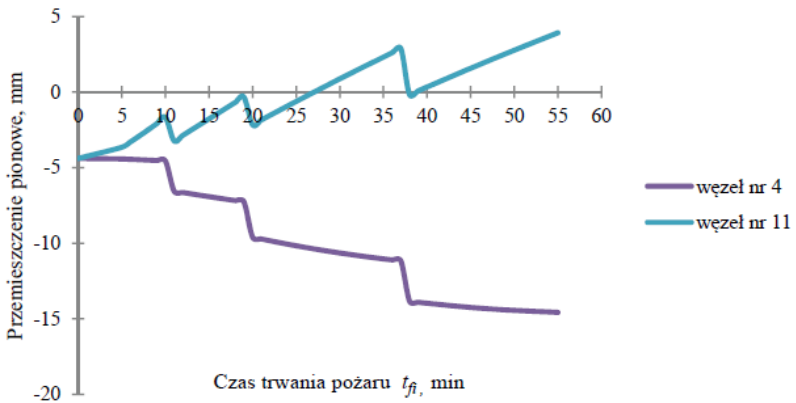

Rys. 4.49. *Zmiana stanu przemieszczeń pionowych centralnych węzłów pasów kratownicy w poszczególnych minutach trwania pożaru*

While the axial forces and resistance variations are determined it is possible to conduct the system reliability assessment.

Basic variables:
cross-sectional areas A, yield stress f_y and load effect E corresponding to distinct members.

Coefficients of variation: $v_A = 6\%$, $v_{fy} = 8\%$, $v_E = 6\%$.

In order to provide system reliability assessment it is necessary to determine the reliability structure, variable in the fire development due to variable static model.

The reliability structure updates each time due to buckling of subsequent structural members.

The following figures show subsequent kinematically admissible failure mechanisms (Polish – KDMZ), given the input truss static model.

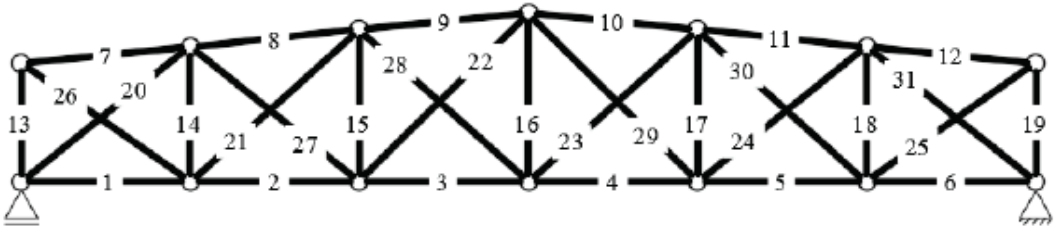
1
2
3
4
5
6
7
8
9
10
11
12
13
14
15
16
17
18
19
20
21
22
23
24
25
26
27
28
29
30
31

I KDMZ

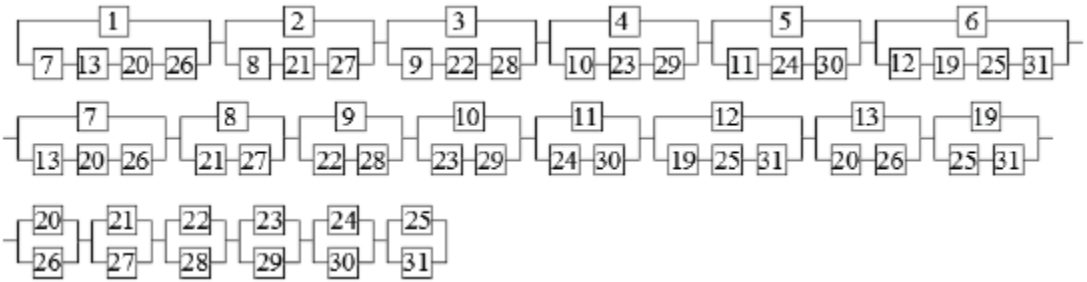
1
7 13 20 26
2
8 21 27
3
9 22 28
4
10 23 29
5
11 24 30
6
12 19 25 31
7
13 20 26
8
21 27
9
22 28
10
23 29
11
24 30
12
19 25 31
13
20 26
19
25 31
20
26
21
27
22
28
23
29
24
30
25
31

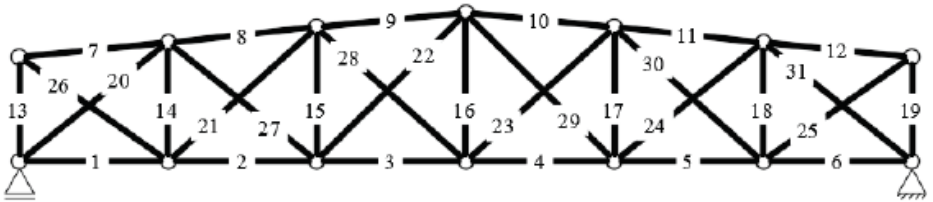

I KDMZ

II KDMZ

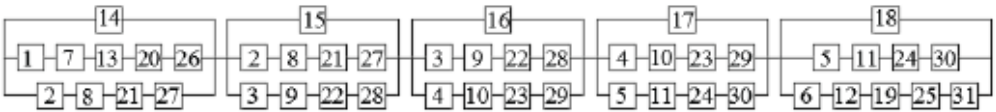

III KDMZ

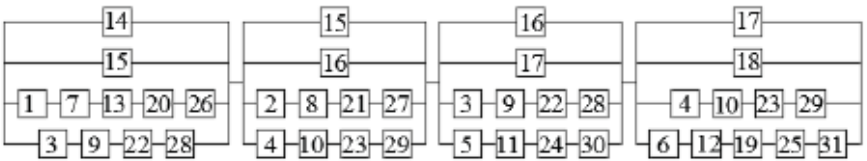

IV KDMZ

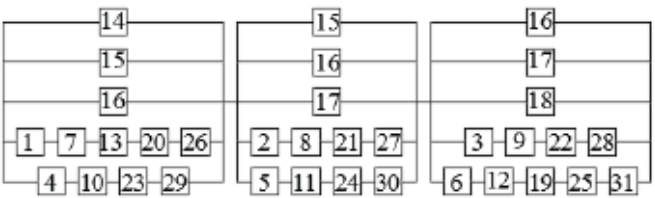

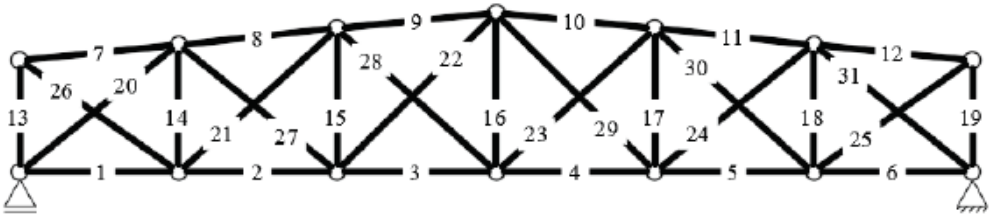

I KDMZ

V KDMZ

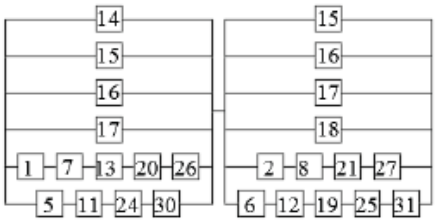

VI KDMZ

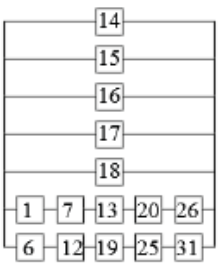

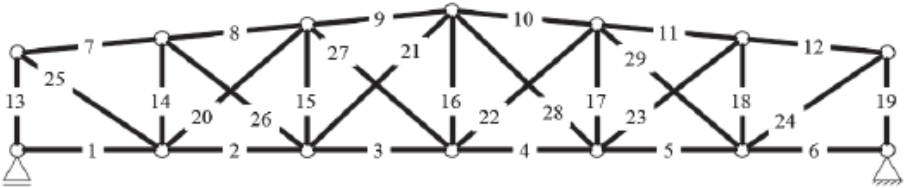

I KDMZ

1 6 7 12 13 19 24 25

II KDMZ

2 — 8 14 20 26
3 — 9 21 27
4 — 10 22 28
5 — 11 18 23 29
8 — 14 20 26
9 — 21 27
10 — 22 28
11 — 18 23 29
14 — 20 26
18 — 23 29
20 — 26
21 — 27
22 — 28
23 — 29

III KDMZ

2 — 15 — 3 9 21 27
3 — 15 — 8 14 20 26
3 — 16 — 4 10 22 28
4 — 16 — 9 21 27
4 — 17 — 5 11 18 23 29
5 — 17 — 10 22 28
8 — 15 — 9 21 27
9 — 15 — 14 20 26
9 — 16 — 10 22 28
10 — 16 — 21 27
10 — 17 — 11 18 23 29
11 — 17 — 22 28
14 — 15 — 21 27
15 — 20 — 21 27
15 — 26 — 21 27
16 — 21 — 22 28
16 — 27 — 22 28
17 — 18 — 22 28
17 — 22 — 23 29
17 — 28 — 23 29

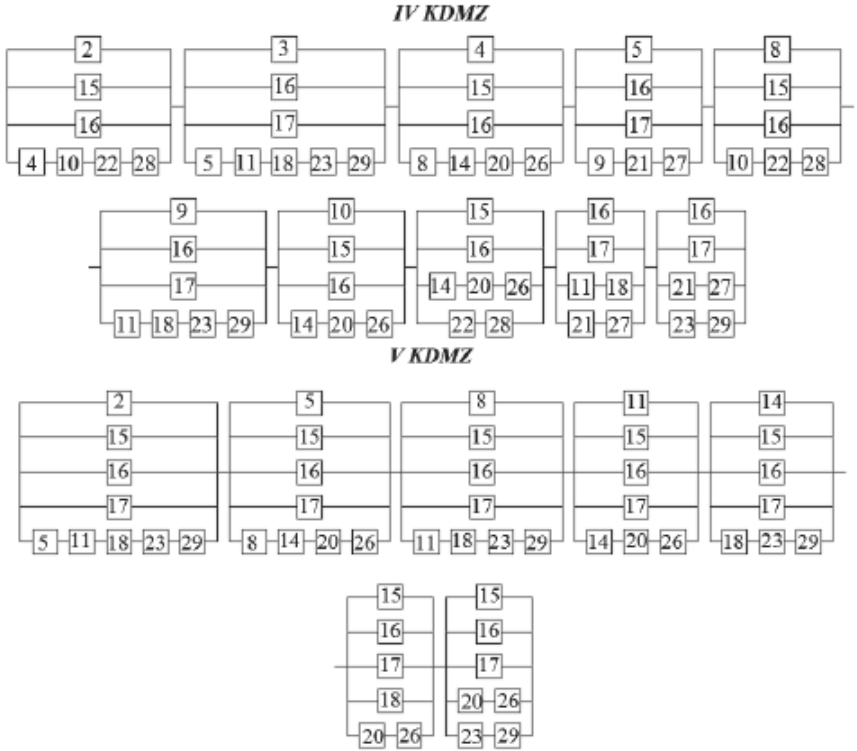
IV KDMZ
2 15 16 4 10 22 28
3 16 17 5 11 18 23 29
4 15 16 8 14 20 26
5 16 17 9 21 27
8 15 16 10 22 28
9 16 17 11 18 23 29
10 15 16 14 20 26
15 16 22 28
16 17 14 20 26 11 18 21 27
16 17 21 27 23 29
V KDMZ
2 15 16 17 5 11 18 23 29
5 15 16 17 8 14 20 26
8 15 16 17 11 18 23 29
11 15 16 17 14 20 26
14 15 16 17 18 23 29
15 16 17 18 20 26
15 16 17 20 26 23 29

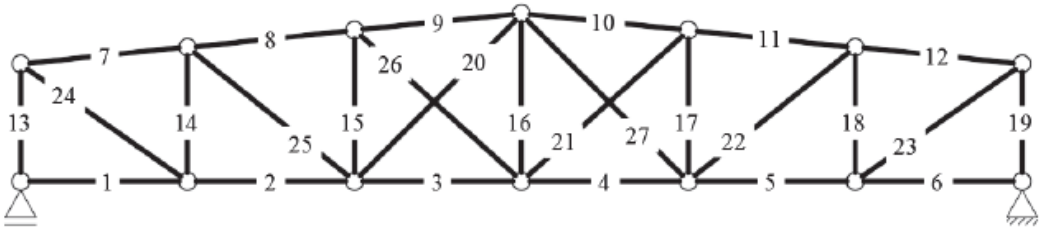

I KDMZ

II KDMZ

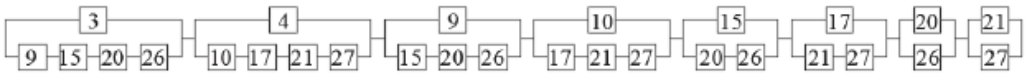

III KDMZ

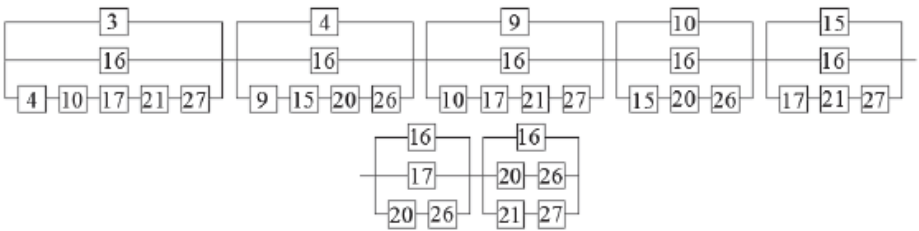

Rys. 4.52. *Kinematycznie dopuszczalne mechanizmy zniszczenia dla kratownicy o schemacie statycznym po drugiej redukcji*

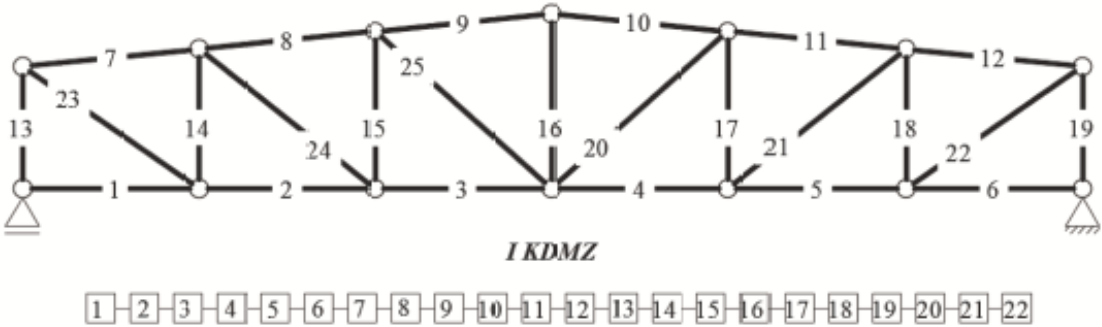

Fig. 4.52. Kinematically allowable failure mechanisms (KDMZ) of a truss, static model after the second reduction

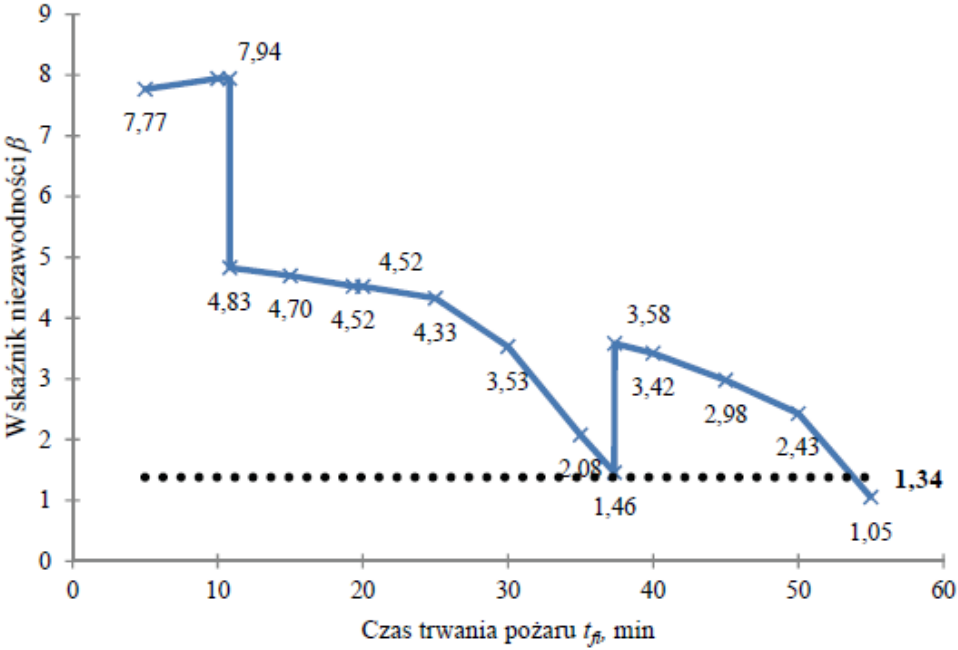

Rys. 4.54. *Zmiana wskaźnika niezawodności kratownicy wielokrotnie statycznie niewyznaczalnej w funkcji czasu trwania pożaru*

Fig. 4.54 Reliability index variation of a truss of multiple degree of static indeterminacy, a function of fire duration t_f